# Mapping the Retina onto the Brain

**Daniel Kerschensteiner[1,2,3] and Marla B. Feller[4,5]**

[1]Department of Ophthalmology and Visual Sciences; [2]Department of Neuroscience; [3]Department of Biomedical Engineering, Washington University School of Medicine, St. Louis, Missouri 63110, USA

[4]Department of Molecular and Cell Biology; [5]Helen Wills Neuroscience Institute, University of California, Berkeley, Berkeley, California 94720, USA

*Correspondence:* mfeller@berkeley.edu; kerschensteinerd@wustl.edu

Cold Spring Harbor Perspectives in Biology
www.cshperspectives.org

Vision begins in the retina, which extracts salient features from the environment and encodes them in the spike trains of retinal ganglion cells (RGCs), the output neurons of the eye. RGC axons innervate diverse brain areas (>50 in mice) to support perception, guide behavior, and mediate influences of light on physiology and internal states. In recent years, complete lists of RGC types (~45 in mice) have been compiled, detailed maps of their dendritic connections drawn, and their light responses surveyed at scale. We know less about the RGCs' axonal projection patterns, which map retinal information onto the brain. However, some organizing principles have emerged. Here, we review the strategies and mechanisms that govern developing RGC axons and organize their innervation of retinorecipient brain areas.

## ORGANIZING PRINCIPLES, LESSER-KNOWN TARGETS, AND POSTSYNAPTIC CHOICES

### Eye-Specific Territories

In mammals, retinal ganglion cell (RGC) axons from both eyes innervate each side of the brain. Contralaterally projecting RGCs (contra-RGCs) occupy the nasal retina, whereas ipsilaterally projecting RGCs (ipsi-RGCs) are found in the temporal retina, which views binocular visual space (Dräger and Olsen 1980). Across species, the decussation line between ipsi- and contra-RGCs moves temporally with more lateral eye positions (Walls 1942; Rodger et al. 1998). Depending on the species, different subsets of RGCs in the temporal retina contribute to the ipsilateral projections (mouse: 20%, cat: 70%, macaque: 100%) (Dräger and Olsen 1980; Illing and Wässle 1981; Fukuda et al. 1989; Johnson et al. 2021). Thus, during development, region- and cell-type-specific sets of RGC axons decide to cross or not to cross at the optic chiasm. In their targets, ipsi- and contra-RGC axons initially overlap but refine to occupy separate territories at maturity (Fig. 1; Godement et al. 1984).

### Retinotopic Maps

Nearby RGCs innervate nearby neurons in their targets to establish topographic maps that maintain spatial information. Like eye-specific territories, retinotopic maps emerge from biased starting points by gradual refinement (Cang and Feldheim 2013). In addition to establishing order among neighboring RGCs, retinotopic maps align visual space across eye-specific territories (Dräger and Hubel 1976; Haustead et al. 2008). During devel-

Editors: Laura C. Andreae, Justus M. Kebschull, and Anthony M. Zador
Additional Perspectives on Evolution and Development of Neural Circuits available at www.cshperspectives.org


Advanced Online Article. Cite this article as *Cold Spring Harb Perspect Biol* doi: 10.1101/cshperspect.a041512

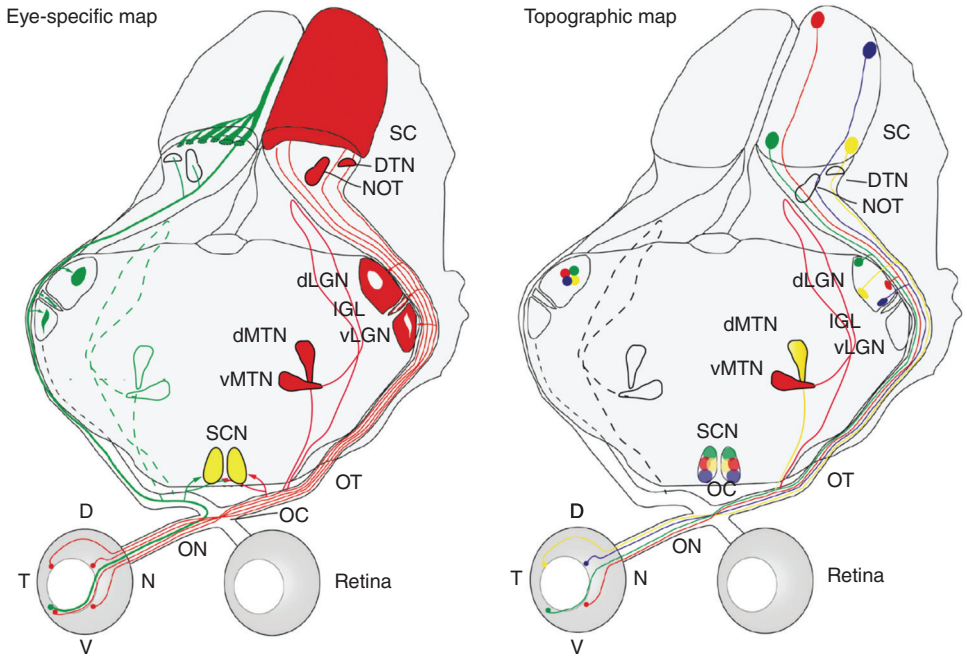


**Figure 1.** Organization of retinal projections into eye-specific territories and topographic maps in the mouse visual system. (ON) Optic nerve, (OC) optic chiasm, (OT) optic tract, (SCN) suprachiasmatic nucleus, (vLGN) ventrolateral geniculate nucleus, (dLGN) dorsolateral geniculate nucleus, (IGL) intergeniculate leaflet; (SC) superior colliculus, (MTN) medial terminal nucleus; (DTN) dorsal terminal nucleus, (NOT) nucleus of the optic tract, (D) dorsal, (N) nasal, (V) ventral, (T) temporal. (Image created from data in Assali et al. 2014.)

opment, retinorecipient targets also register ascending inputs from the retina with descending visual inputs (Rhoades and Chalupa 1978) and, in the superior colliculus (SC), other sensory modalities and motor outputs (Schiller and Stryker 1972; Wurtz and Goldberg 1972; Sparks et al. 1990; Knudsen and Brainard 1995; Triplett et al. 2012).

## Type-Specific Targets and Layers

Neurons can be classified into types based on their morphology, gene expression pattern, and function (Zeng and Sanes 2017). Large-scale surveys of each modality identified similar numbers of RGC types (~45) in mice (Baden et al. 2016; Bae et al. 2018; Rheaume et al. 2018; Tran et al. 2019). Recent multimodal analyses revealed good correlation between the unimodal classification schemes and identified cross-modal correspondences (Goetz et al. 2022; Huang et al. 2022). Each of the mouse's ~45 RGC types sends its unique feature representation of the world to a specific subset of >50 retinorecipient brain areas (Morin and Studholme 2014; Martersteck et al. 2017; Kerschensteiner 2022). The same applies, with different numbers, to other species (e.g., macaques: ~18 RGC types and >20 retinorecipient areas) (Hendrickson et al. 1970; O'Brien et al. 2001; Dacey 2004; Peng et al. 2019). Most brain targets receive input from multiple RGC types, whose axons occupy type-specific layers in the target (Reese 1988; Huberman et al. 2009; Hong et al. 2011, 2019; Tien et al. 2022). In addition to choosing the right targets and correct layers, developing RGC axons replicate topographic maps in each type-specific layer and repeat layers across eye-specific territories (Cang and Feldheim 2013).

## Lesser-Known Targets

The principles of RGC axon organization (i.e., eye-specific territories, retinotopic maps, and

type-specific layers) were gleaned from studies of the two main retinorecipient targets in mammals: the dorsolateral geniculate nucleus (dLGN) of the thalamus and SC (Kerschensteiner and Guido 2017; Cang et al. 2018; Liang and Chen 2020). To what extent these principles and the mechanisms that control RGC axon organization are preserved across targets is unclear. In addition to dLGN and SC, this review summarizes recent insights into the RGC innervation of the lesser-known majority of targets.

### Postsynaptic Choices

RGC axons lay out retinal information according to the principles described above. How this information is used (e.g., whether retinal representations are preserved downstream or combined to extract new features) depends on the dendritic sampling of these maps by postsynaptic target neurons. Morphological, transcriptomic, and functional surveys are beginning to define the diversity of postsynaptic neurons in retinorecipient targets (Krahe et al. 2011; Piscopo et al. 2013; Gale and Murphy 2014; Reinhard et al. 2019; Bakken et al. 2021; Liu et al. 2023b). We cover postsynaptic contributions to retina-to-brain mapping where they are known.

## RETINAL WAVES

Retinal connectivity to the brain is established early in development. RGC axons reach their targets before birth and long before photoreceptors drive their responses (Wong 1999). Although guidance cues and molecular interactions are critical for this process, as RGCs innervate their targets, they are also spontaneously active. This spontaneous activity occurs in waves propagating across the developing retina (i.e., retinal waves). Retinal waves provide a robust source of depolarization and correlated activity to the retina and downstream visual areas, including the SC, dLGN, and primary visual cortex (V1) (Kirkby et al. 2014; Seabrook et al. 2017). Waves emerge in a retina with few synapses and a large ventricular zone populated by precursor cells (embryonic day E16 in mice) (Catsicas et al. 1998; Bansal et al. 2000) and persist until eye opening (postnatal day P14 in mice) when all neurons have differentiated and synaptic circuits are nearly mature (Fisher 1979; Demas et al. 2003; Kerschensteiner 2020). Although there is a continuum of changes, retinal waves are typically classified into three stages (1–3), in which different circuit mechanisms generate waves with distinct activity patterns. Waves have mostly been studied in isolated retinas, but recent calcium imaging of RGC axons in the SC confirmed their existence in vivo and revealed similar spatiotemporal patterns (Ackman et al. 2012; Ackman and Crair 2014).

Retinal waves have been observed in many species, including primates (Wong 1999; Warland et al. 2006), but are best studied in mice. During stage 1 (E16-P1 in mice), retinal waves are characterized by two types of events: small nonpropagating events and large propagating ones (Bansal et al. 2000; Voufo et al. 2023). Both events are blocked by nicotinic acetylcholine receptor (nAChR) antagonists; the large propagating events are also blocked by gap junction antagonists (Voufo et al. 2023). Thus, stage 1 waves are mediated by a combination of electrical synapses, likely among specific RGC types, and volume transmission of ACh. During stage 2 (P2-P10 in mice), waves propagate across large distances, only limited by refractory periods induced by a previous wave (Ford et al. 2012). During this stage, all waves are blocked by nAChR antagonists and are mediated by volume transmission of ACh. The transition to stage 3 waves occurs as glutamatergic bipolar cell synapses in the inner retina mature (P11-P13 in mice) (Fisher 1979; Morgan et al. 2008; Akrouh and Kerschensteiner 2013; Kerschensteiner 2016). Stage 3 waves are unaffected by nAChR antagonists and are blocked by ionotropic glutamate receptor antagonists. Stage 3 waves have more complex propagation patterns and cover shorter distances than their predecessors (Kerschensteiner and Wong 2008; Gribizis et al. 2019; Ge et al. 2021). Interestingly, stage 3 waves can be triggered by photoreceptor activation, allowing light to enter through the closed eyelids to influence spontaneous activity patterns (Tiriac et al. 2018). During late stage 2 and early stage 3, waves exhibit a propagation bias, with more waves prop-

agating in the nasal direction in retinal coordinates, mimicking the optic flow generated when mice move forward (Stafford et al. 2009; Elstrott and Feller 2010; Ge et al. 2021; Tiriac et al. 2022).

## BINOCULAR VISION

Mammalian brains integrate information from both eyes to extract depth cues (i.e., stereopsis) and enhance visual sensitivity in the frontal visual field (Read 2021). To support binocular integration in the brain, most RGCs cross at the optic chiasm (i.e., contra-RGCs), but some innervate ipsilateral targets (i.e., ipsi-RGCs). This section reviews the development of contra- and ipsi-RGCs, the factors that guide their axons at the chiasm and shape their terminal arbors in retinorecipient targets.

### Ipsi- and Contralaterally Projecting RGCs

Ipsi-RGCs are found in the temporal crescent of the mouse retina (Dräger and Olsen 1980). Retrograde tracing revealed that only a subset (~20%) of RGCs in the temporal retina innervate ipsilateral brain targets (Dräger and Olsen 1980), and a functional and morphological survey showed that ipsi-RGCs comprise nine of the ~45 RGC types in mice (Johnson et al. 2021).

The decision to cross or not at the optic chiasm is guided by molecular interactions between cues presented by radial glia and early-born neurons at the diencephalic midline and receptors on RGC axons (Mason and Slavi 2020). Thus, radial glia and midline neurons express ephrin-B2, which interacts with EphB1 receptors on ipsi-RGC axons, repelling them from the midline (Williams et al. 2003; Petros et al. 2010). Conversely, several pairs of midline ligands and axonal receptors (i.e., Semaphorin6D-PlexinA1, NrCAM-NrCAM, VEGF-A-Neuropilin 1) attract contra-RGC axons to the midline and promote their crossing (Williams et al. 2006; Erskine et al. 2011; Kuwajima et al. 2012). Repulsive signals from contra-RGCs, releasing Sonic hedgehog (Shh), to ipsi-RGCs, expressing the Shh-receptor Boc, further segregate their axons in the optic chiasm (Sánchez-Arrones et al. 2013; Peng et al. 2018).

Transcriptional programs differentiating ipsi- and contra-RGCs have been uncovered. The Zinc finger transcription factor Zic2 is restricted to ipsi-RGCs across species, including mice (Herrera et al. 2003). It determines the path of their axons by driving the expression of EphB1 receptors (García-Frigola et al. 2008; Lee et al. 2008) and the Shh-receptor Boc (Fabre et al. 2010; Sánchez-Arrones et al. 2013). Transcription factors associated with contra-RGCs include Islet2, Brn3a, and SoxC (Mason and Slavi 2020). Clear links from these transcription factors to axon guidance remain to be established.

Albinism, including in humans, is associated with a reduced ipsilateral RGC projection (Prieur and Rebsam 2017; Kruijt et al. 2018). Recent findings indicate that the down-regulation of CyclinD2 in the ciliary marginal zona (a neurogenic niche) of albino mice prolongs the $G_1$/S phase transition in the progenitor cell cycle, compromising the generation of ipsi-RGCs (Slavi et al. 2023).

### Eye-Specific Organization in dLGN

In mice, ipsi-RGC axons innervate a dorsomedial patch of the dLGN that contra-RGC axons avoid (Rafols and Valverde 1973). During development, the position of the ipsilateral patch is defined by molecular cues and the segregation of ipsi- and contra-RGC axons is driven by activity-dependent mechanisms.

Ephrin-As and EphA receptors mediate repulsive interactions and are expressed in complementary gradients in the dLGN and the retina, respectively (Feldheim et al. 1998). Conversely, Ten_m3, a cell-adhesion molecule that mediates homophilic attraction, is expressed in matching gradients in the dLGN and the retina (Leamey et al. 2007). Disruption of either set of gradients disperses the termination zones of ipsi-RGC axons, whereas activity-dependent refinement drives their segregation from contra-RGCs, resulting in fragmented and displaced ipsi-RGC patches in dLGN (Huberman et al. 2005; Pfeiffenberger et al. 2005; Leamey et al. 2007).

The extracellular glycoprotein Nell2 localizes to the ipsilateral patch of dLGN and repels contra-RGC axons. Deletion of Nell2 results in

an invasion of contra-RGCs, particularly in the caudal dLGN, and, after activity-dependent refinement, a similar fragmentation and dispersion of the ipsi-RGC projection to the gradient disruptions (Nakamoto et al. 2019).

The axons of ipsi- and contra-RGCs initially overlap and are gradually separated during development (between postnatal days 4 and 10 in mice) (Rossi et al. 2001; Muir-Robinson et al. 2002). Eye-specific segregation coincides with the period of stage 2 waves, and deleting the β2-subunit of nAChRs (i.e., β2-nAChR-KO mice), which significantly reduces stage 2 waves, prevents eye-specific segregation (Rossi et al. 2001; Muir-Robinson et al. 2002; Burbridge et al. 2014). Retinal waves correlate the activity of RGCs in each eye. Because stage 2 waves are short compared to their intervals and occur independently in the two eyes, wave activity can drive eye-specific segregation via correlation-based synaptic plasticity rules (e.g., burst-time-dependent plasticity) (Butts et al. 2007). Optogenetic stimulation demonstrated the importance of asynchronous activity in segregating ipsi- and contra-RGC axons in dLGN (Zhang et al. 2011). Activity-dependent synaptic plasticity promotes competition, and when ipsi-RGCs are silenced, they fail to expel contra-RGC axons from their dLGN territories (Penn et al. 1998; Koch and Ullian 2010; Koch et al. 2011).

Thus, retinal waves drive and maintain (Demas et al. 2006) the eye-specific segregation of RGC axons in territories whose position in dLGN is molecularly defined.

The small size of the ipsi-RGC axon patch compared to the thalamocortical (TC) neuron dendrite arbors means that ipsi- and contra-RGCs could converge onto TC neurons (Krahe et al. 2011). Indeed, monosynaptic rabies virus tracing found frequent binocular convergence (Rompani et al. 2017), and in vivo recordings identified TC neurons responding to visual stimulation through either eye (Howarth et al. 2014). However, TC neurons restrict strong RGC inputs to their proximal dendrites (Morgan et al. 2016), and optogenetic experiments revealed that when ipsi- and contra-RGCs converge, one eye's input is strongly dominant, and the other eye's input is arrested in synaptic development (Bauer et al. 2021). Thus, the choices made by the postsynaptic neurons largely maintain the functional separation established by the eye-specific segregation of RGC axons.

## Eye-Specific Organization in SC

Ipsi- and contra-RGC inputs to the superficial SC (sSC) are laminarly separated. Ipsi-RGC axons stratify in the deepest layer of sSC (i.e., the stratum opticum [SO]), whereas contra-RGCs target the upper layers (i.e., stratum griseum superficiale [SGS] and stratum zonale [SZ]) (Godement et al. 1984; Hong et al. 2011). Unlike the gradual refinement in dLGN, ipsi-RGC axons are restricted to SO from the outset (García-Frigola and Herrera 2010). Su et al. (2021) showed that the extracellular glycoprotein nephronectin is limited to the SO and is required for its ipsi-RGC innervation. This positional cue is produced by wide-field neurons in SC, whose cell bodies reside in SO (Tsai et al. 2022). Ipsi-RGC axons express α8β1 integrin, which binds nephronectin and guides them to their laminar target (Su et al. 2021).

Although molecular cues establish eye-specific axon segregation in SC, retinal waves are required for its maintenance. Thus, ipsi-RGCs begin to stray into SGS and SZ in β2-nAChR-KO mice (Rossi et al. 2001; Burbridge et al. 2014) or when the activity of both eyes is optogenetically synchronized (Zhang et al. 2011).

The extent of binocular convergence in SC is still unclear. A recent characterization of light responses revealed complex interactions between stimuli presented through both eyes (Russell et al. 2022), which could be indirect. Moreover, how binocular convergence differs between different SC neuron types remains to be determined (Gale and Murphy 2014; Tsai et al. 2022; Liu et al. 2023b).

## Eye-Specific Organization in Lesser-Known Targets

Most retinorecipient targets receive input from both eyes (Morin and Studholme 2014; Martersteck et al. 2017). The extent of ipsilateral input depends on the complement of RGC types in-

nervating each target. For example, nuclei of the accessory optic system (i.e., the medial terminal nucleus [MTN], dorsal terminal nucleus [DTN], and nucleus of the optic tract [NOT]), which mediate the gaze-stabilizing optokinetic reflex, receive limited ipsilateral input because their retinal innervation is dominated by ON direction-selective (DS) RGCs, which are excluded from the ipsi-RGC set (Simpson 1984; Gauvain and Murphy 2015; Johnson et al. 2021). By contrast, the olivary pretectal nucleus (OPN), which mediates the pupillary light response (i.e., the pupil's constriction to increasing light levels), receives abundant input from M1 and M6 intrinsically photosensitive RGCs (ipRGCs), which are overrepresented in the ipsi-RGC set (Hattar et al. 2006; Levine and Schwartz 2020; Johnson et al. 2021). The M1 ipRGC population encodes global luminance in a distributed manner, and its ablation abolishes the pupillary light response (Chen et al. 2011; Milner and Do 2017; Liu et al. 2023a). Eye-specific axon segregation in OPN appears precise from the outset (McNeill et al. 2011); the mechanisms guiding this organization remain unknown.

Across species, the size of ipsilateral projections can be predicted from the eye positions: the more lateral the eyes, the smaller the ipsilateral projection (i.e., the Newton–Müller–Gudden law) (Walls 1942). The retinal projection to the suprachiasmatic nucleus (SCN), which entrains circadian rhythms to light, consistently breaks this law (Magnin et al. 1989). The SCN is predominantly innervated by M1 ipRGCs (Hattar et al. 2006; Baver et al. 2008; Güler et al. 2008). Single-cell labeling demonstrated that the axons of individual M1 ipRGCs frequently innervate both SCNs via collaterals branching at the chiasm or within the SCN (Fernandez et al. 2016). As a result, the mouse SCN receives approximately equal input from both eyes (Hattar et al. 2006; Fernandez et al. 2016). However, functional convergence appears limited, and 67% of cells respond exclusively to stimuli through one or the other eye (Walmsley and Brown 2015). Unlike dLGN and SC (Howarth et al. 2014; Russell et al. 2022), monocular responses in SCN are equally distributed between ipsi- and contralateral eyes (Walmsley and Brown 2015). The mechanisms guiding the development of bilateral axonal projections and maintaining postsynaptic eye-specific segregation in SCN remain to be uncovered.

## RETINOTOPY

Nearby RGCs innervate nearby neurons in retinorecipient targets to maintain spatial information. This section reviews regional specializations within the retina and the mechanisms that establish and refine retinotopic target innervation.

### Regional Specializations of RGCs

Most RGCs are distributed across the retina in regular mosaics, in which the distances between same-type neighbors are relatively constant. This arrangement enables the retina to encode visual features uniformly across space. However, recent experiments have revealed striking variations in RGC density and receptive field properties across the mouse retina (i.e., regional specializations) (Rivlin-Etzion et al. 2018; El-Danaf and Huberman 2019; Heukamp et al. 2020).

The retinas of many species contain areas in which the RGC density is increased and dendritic and receptive fields are proportionally smaller, allowing for high-acuity vision (i.e., acute zones) (Baden et al. 2020). When all RGCs are labeled, no acute zones are visible in the mouse retina (Dräger and Olsen 1981). However, Bleckert et al. (2014) discovered that the density of sustained ONα and OFFα RGCs, which signal local light increments and decrements (i.e., luminance contrast), respectively, is elevated, and their dendritic and receptive fields are smaller in the temporal retina, forming a cell-type-specific binocular acute zone. An extreme asymmetry in distribution has also been observed in the non-image-forming pathway, where a subtype of M1 ipRGCs resides exclusively in the dorsal retina and projects to specific targets within the SCN, the supraoptic nucleus through which light regulates metabolism and social memories, and the zona incerta, a structure associated with novelty seeking and the integration of sensory and motivational cues for

predation (Zhao et al. 2019; Monosov et al. 2022; Berry et al. 2023; Huang et al. 2023; Meng et al. 2023).

In addition, regional specializations in RGC function have been identified. Thus, the responses of transient Offα RGCs are more sustained in the dorsal than the ventral retina (Warwick et al. 2018). Transient OFFα RGCs in the ventral retina drive the innate defensive responses of mice to looming stimuli that signal approaching aerial predators in the sky (Münch et al. 2009; Kim et al. 2020; Wang et al. 2021). Furthermore, variations in the center-surround organization of receptive fields have been observed across multiple RGC subtypes that appear optimized to encode variations in spatiotemporal features of natural scenes across the visual field (Gupta et al. 2023). The developmental bases of these regional specializations in cell density and function have not yet been elucidated.

The preferred directions of DS RGCs vary with location in the retina, following a coordinate system defined by optic flow (Sabbah et al. 2017; Tiriac et al. 2022). Thus, the preferred directions of horizontal DS RGCs converge on a singularity in the temporal retina, from which optic flow emerges when mice move forward. Vertical DS RGC preferences converge on a ventral singularity. The mapping of horizontal but not vertical DS RGC motion preferences depends on retinal waves, which show a horizontal propagation bias aligned with optic flow fields during late stage 2 and early stage 3 (Stafford et al. 2009; Elstrott and Feller 2010; Sabbah et al. 2017; Ge et al. 2021; Tiriac et al. 2022).

## Retinotopic Organization in dLGN

Contra-RGCs are organized retinotopically, with the nasal–temporal retinal axis mapping onto the ventrolateral–dorsomedial axis of the dLGN, and the dorsoventral retinal axis mapping onto the ventromedial–dorsolateral axis of the dLGN (Lund et al. 1974). Ipsilaterally projecting axons also follow a retinotopic organization with ventrotemporal RGCs projecting to the dorsal part of the ipsi-recipient region, which is shifted ventrally from the contra-RGC axons. Ephrin-A/EphA interactions guide nasotemporal mapping, with high ephrin ligand expression in ventrolateral anterior dLGN (Pfeiffenberger et al. 2005). Mice lacking ephrin-As exhibit abnormal mapping along this axis, although the defects are less dramatic than in the SC (Pfeiffenberger et al. 2005). Also, in contrast to SC, there are no overshooting axons but increased branching in the correct retinotopic location (Dhande et al. 2011; Assali et al. 2014). Knocking out ephrin-A signaling and retinal waves leads to the most dramatic disruption along the horizontal visual field axis (Pfeiffenberger et al. 2006). Reconstructions of individual retinogeniculate axons showed that activity disruption prevents the refinement of their arbors (Dhande et al. 2011; Benjumeda et al. 2013).

After eye-opening, retinotopic connections between RGCs and TC neurons continue to refine, a process driven by visual experience (Hooks and Chen 2006, 2008).

## Retinotopic Organization in SC

The mechanisms underlying the development of retinotopic maps have been most intensely studied in the contra-RGC projections to the SC (Triplett and Feldheim 2012; Cang and Feldheim 2013; Johnson and Triplett 2021; Tomar et al. 2023). In mice, contra-RGC axons reach the rostral end of the SC at E16 and grow across to the caudal end by P2. Over the first postnatal week, overshooting branches are retracted, and axons elaborate dense arbors in their final termination zone (Simon and O'Leary 1992; Yates et al. 2001). Distinct mechanisms appear to determine the size and location of the termination zone along the rostrocaudal axis versus the mediolateral axis, which represents the vertical visual field.

The retraction of overshooting branches and the location of the termination zone along the rostrocaudal axis are determined by contact-mediated repulsive interactions between ephrin-As and EphA receptors and retinal waves. Temporal RGCs with high receptor expression are strongly repelled from caudal SC, whereas nasal RGC axons with lower receptor expression are less sensitive to high ligand concentrations, and so remain. This model is supported by loss-of-function and gain-of-function studies (Nakamoto et al. 1996; Frisén et al. 1998; Feldheim et al.

2000; Cang et al. 2008). Single knockout mice have minor retinotopic defects, often manifesting as a normal projection with an ectopic termination zone, with more serious deficits associated with double and triple mutants, indicating it is the sum total of ephrin-A/EphA signaling, rather than specific ephrin-A/EphA receptor species that drive repulsion (Cheng et al. 1995; Triplett and Feldheim 2012). More recent studies based on conditional knockouts of ephrin-A5 in the retina indicate that SC-independent ephrin-A/EphA interactions between RGC axons also contribute to their topographic mapping (Suetterlin and Drescher 2014). A role for axon–axon interactions is also supported by a study in which the depletion of large percentages of RGCs led to the degradation of retinotopic maps (Maiorano and Hindges 2013).

Waves also contribute to the retinotopic mapping of RGC axons to SC. In β2-nAChR-KO mice or mice in which waves have been inhibited pharmacologically, axonal arbors are centered on the correct retinotopic locations but with expanded termination zones (McLaughlin et al. 2003; Burbridge et al. 2014). These expanded termination zones expand receptive fields in SC (Chandrasekaran et al. 2005; Mrsic-Flogel et al. 2005). Knocking out both β2-nAChRs and ephrin-As leads to a complete lack of refinement along the horizontal visual axis (Pfeiffenberger et al. 2006).

Refinement along the vertical visual axis (dorsoventral on the retina, mediolateral in the SC) follows a different developmental program. When entering the SC, RGC axons are partially organized along the mediolateral axis, branching off the primary axon in the correct termination zones (Plas et al. 2005). EphB/ephrin-B have counter gradients within the retina and SC. Loss-of-function and overexpression studies imply that targeting of these axonal branches depends on EphB/ephrinB interactions, although the details remain obscure (Hindges et al. 2002). Other molecular gradients have also been implicated, including Wnt signaling (Schmitt et al. 2006) and cell-adhesion molecules (Dai et al. 2013). Activity manipulations have limited effects along this axis, indicating that it is likely to be mediated primarily by guidance molecules.

## Retinotopic Alignment of Feedforward and Feedback Connections in SC and dLGN

The SC and the dLGN receive feedback connections from V1 that are retinotopically organized and aligned with feedforward retinal inputs (Triplett et al. 2009; Wang and Burkhalter 2013). Descending cortical inputs appear to modulate the gain of SC neuron responses but not alter the feature preferences they inherit from the retina (Zhao et al. 2014; Liang et al. 2015; Cang et al. 2018). Following RGC innervation and refinement in the first postnatal week, axons from layer 5 neurons in V1 reach SC starting at P6 and refine their termination zones by P12 in alignment with the retinal input map. The topographic refinement of the cortical input is instructed by the retinal projection (Johnson and Triplett 2021) and depends on ephrin-A gradients (Savier et al. 2017) and activity (Triplett et al. 2009). Interestingly, the refinement of V1 projections but not retinal projections to SC depends on postsynaptic NMDA receptors (Johnson et al. 2023).

The dLGN receives input from layer 6 of V1, which is also aligned with the retinal input (Hasse and Briggs 2017). Layer 6 axons arrive in the dLGN around P0 but only innervate the nucleus after the retinal input has traversed the structure at P3. The cortical innervation of dLGN is accelerated in the absence of RGC input (Seabrook et al. 2013), a process modulated by neural activity (Moreno-Juan et al. 2023). Corticogeniculate feedback also regulates the experience-dependent refinement of retinogeniculate synapses after eye-opening (Thompson et al. 2016).

## Retinotopic Organization in Lesser-Known Targets

In retinorecipient regions, other than dLGN and SC, the development of topographic organization has rarely been explored (Dhande et al. 2015). Inputs to the ventrolateral geniculate nucleus (vLGN), which may mediate a wide range of light influences on mood, learning, and behavior (Huang et al. 2019, 2021; Fratzl et al. 2021; Salay and Huberman 2021; Hu et al. 2022), arrive in the first postnatal week (Su et al. 2011), are

organized retinotopically (Holcombe and Guillery 1984), and undergo eye-specific segregation (Monavarfeshani et al. 2017). The mechanisms that govern this organization remain unexplored.

In the SCN, which receives overlapping ipsilateral and contralateral inputs from M1 ipRGCs, there is some evidence for a coarse retinotopic organization (Fernandez et al. 2016). The limited retinotopic and eye-specific refinement in the SCN may partly be due to the lack of M1 ipRGC participation in retinal waves (Caval-Holme et al. 2022).

## TYPE-SPECIFIC PATHWAYS

The retina extracts salient features from the environment and encodes them in the spike trains of diverse RGC types (~45 in mice). RGCs innervate an equally diverse set of brain areas (>50 in mice) to guide actions, generate perception, and mediate influences of light on physiology (Morin and Studholme 2014; Martersteck et al. 2017). This section reviews how developing RGCs choose specific targets, how they organize their axons within, and how postsynaptic neurons select inputs from the diverse RGC offering.

### Type-Specific RGC Projections

The number of targets varies widely between RGC types; some innervate one or two brain areas (Chen et al. 2011; Martersteck et al. 2017), whereas others innervate more than 10 (Hattar et al. 2006). Screens of transgenic mice revealed that single drivers, with few exceptions, label several RGC types (Siegert et al. 2009; Ivanova et al. 2010; Badea and Nathans 2011; Martersteck et al. 2017), and isolating individual RGC types requires intersectional strategies (Chen et al. 2011; Tien et al. 2022). A few studies have labeled single RGCs and shown that their axons innervate multiple targets via collaterals, forming complete retinotopic maps in each (Dhande et al. 2011; Fernandez et al. 2016).

Different developmental strategies for target innervation have been identified. ON–OFF DS RGC axons innervate the correct targets shortly after they arrive in the brain postnatally. Conversely, transient suppressed-by-contrast (tSbC) RGCs span the length of the optic tract by birth and remain poised there until they simultaneously innervate their four targets (i.e., dLGN, vLGN, SC, and NOT) around P3. Like ON–OFF DS RGCs, tSbC RGCs make no developmental errors in their target choices. The same applies to M1 ipRGCs (McNeill et al. 2011). By contrast, M6 ipRGCs have been reported to explore more targets during development than they keep at maturity. However, developmental changes in the labeling specificity of the Cdh3-GFP transgenic mice used to trace M6 ipRGC projections in this study indicate that this developmental deviation needs to be reevaluated (Osterhout et al. 2011, 2014; Quattrochi et al. 2019). Whether these different developmental strategies correlate with particular features of these RGC types or their targets remains to be determined.

Molecular mechanisms that guide RGC-type-specific target choices are discussed in the following sections.

### RGC-Type-Specific Organization in dLGN

In primates, cats, and ferrets, dLGN neurons are divided into layers that get input from specific RGC types (Usrey and Alitto 2015; Liang and Chen 2020). Mice and rats lack clear separation in dLGN neurons, but RGC projections divide the dLGN into a dorsolateral shell and ventromedial core (Reese 1988). More than 30 mouse RGC types innervate the dLGN (Ellis et al. 2016; Román Rosón et al. 2019). The shell receives input from ON–OFF DS RGCs, orientation-selective RGCs, and F RGCs (Kim et al. 2008; Huberman et al. 2009; Kay et al. 2011; Rivlin-Etzion et al. 2011; Rousso et al. 2016; Nath and Schwartz 2017). The core is strongly innervated by α RGCs, $Pix_{ON}$ RGCs, ipRGCs, and transient suppressed-by-contrast RGCs (Huberman et al. 2008; Ecker et al. 2010; Johnson et al. 2018; Tien et al. 2022). TC neurons in the dLGN shell and core innervate layers 1/2 and 4 of V1, respectively (Cruz-Martín et al. 2014), extending the parallel visual pathways from the retina. The shell and core contain complete retinotopic maps (Reese 1988). Eye-specific segregation is limited to the core (Liang and Chen 2020) because the

RGC types targeting the shell lack ipsilateral projections (Johnson et al. 2021). The mechanisms that guide RGC types to the dLGN shell or core remain unknown.

TC neurons initially receive weak input from many RGCs and consolidate and strengthen connectivity with synaptic partners across development (Chen and Regehr 2000; Liang and Chen 2020). Estimates of mature convergence (i.e., how many RGCs innervate each TC neuron) vary by technique and between target cells, but, on average, TC neurons receive input from ~10 RGCs (Chen and Regehr 2000; Hammer et al. 2015; Morgan et al. 2016; Litvina and Chen 2017; Rompani et al. 2017; Román Rosón et al. 2019).

The refinement of RGC–TC connections depends on spontaneous activity (Hooks and Chen 2006). In addition to correlating RGC activity in a distance-dependent manner, stage 3 waves desynchronize the activity of neighboring RGCs with opposite light responses (ON vs. OFF) (Kerschensteiner and Wong 2008; Akrouh and Kerschensteiner 2013). Given burst-time-dependent plasticity rules (Butts et al. 2007), the asynchronous activation of nearby ON and OFF RGCs is predicted to separate their innervation in retinotopically refined projections (Kerschensteiner and Wong 2008; Gjorgjieva et al. 2009). In ferrets, blocking stage 3 waves blocks ON/OFF segregation (Hahm et al. 1991; Cramer and Sur 1997), and mice with precocious stage 3 waves show excessive ON/OFF segregation (i.e., ON and OFF dLGN neurons, which normally intermingle, congregate separately) (Grubb et al. 2003).

At a fine scale (~6 µm), boutons of RGC axons with overlapping feature preferences (including ON vs. OFF responses and motion direction preferences) cluster to converge onto TC neurons (Liang et al. 2018). The formation of complex bouton clusters depends on Lrrtm1, a postsynaptic cell-adhesion molecule on TC neuron dendrites (Monavarfeshani et al. 2018). The organization of synaptic boutons within RGC axons is also shaped by visual experience and late dark rearing (i.e., from postnatal day 20 to 30) disperses clustered boutons and reduces their size (Hong et al. 2014).

Like TC neurons, local interneurons (LINs) in dLGN receive input from diverse RGC types (Morgan and Lichtman 2020; Muellner and Roska 2023). RGC convergence appears to be higher for LINs than TC neurons. Individual LINs select input from nonrandom sets of RGC types to preserve feature-selective responses, similar to TC neurons (Piscopo et al. 2013; Muellner and Roska 2023). The mechanisms that regulate RGC connectivity with dLGN LINs remain to be elucidated.

## RGC-Type-Specific Organization in SC

More than 85% of mouse RGCs project to sSC (Ellis et al. 2016). Transgenic labeling of specific RGC populations and viral labeling of individual cells revealed that axons of different RGC types stratify at particular depths within the sSC (Huberman et al. 2008, 2009; Kim et al. 2008; Hong et al. 2011; Tien et al. 2022). Whereas some RGC axons target the correct depths from the outset (Kim et al. 2010; Tien et al. 2022), others establish mature patterns gradually (Huberman et al. 2008; Kim et al. 2010). The molecular or activity-dependent mechanisms that guide developing RGC axons to specific SC depths remain to be uncovered.

The sSC contains different neuron types that can be distinguished by their dendritic morphology, axonal projection patterns, visual functions, and gene expression (Gale and Murphy 2014; Tsai et al. 2022; Li and Meister 2023; Liu et al. 2023b). Synaptic physiology suggests that each SC neuron receives input from ~5 RGCs (Chandrasekaran et al. 2007). The observation that molecularly distinct SC neuron types differ in their functional responses, therefore, suggests that SC neurons select input from specific RGC types (Gale and Murphy 2014; Hoy et al. 2019; Liu et al. 2023b), a notion supported by retrograde tracing and transsynaptic sequencing experiments (Reinhard et al. 2019; Tsai et al. 2022). Connections between ipsilaterally projecting αRGCs and wide-field neurons in SC depend on α8β1 integrin expression of the RGC axons and nephronectin production by the target (Su et al. 2021; Tsai et al. 2022). The comprehensive transcriptomic data sets available on both sides

should accelerate the discovery of molecular partners that match RGC and SC neuron types (Rheaume et al. 2018; Tran et al. 2019; Dimitrov et al. 2022; Tsai et al. 2022; Liu et al. 2023b).

Whether RGC-type-specific connectivity patterns vary across SC topography to form feature maps for motion direction and stimulus orientation and, if so, what drives the development of these maps are matters of ongoing debate and investigation (Ahmadlou and Heimel 2015; Feinberg and Meister 2015; de Malmazet et al. 2018; Li et al. 2020; Chen et al. 2021; Ge et al. 2021; Tiriac and Feller 2022; Tiriac et al. 2022).

## RGC-Type-Specific Innervation of Lesser-Known Targets

M1 ipRGCs strongly innervate the vLGN and the intergeniculate leaflet (IGL) of the visual thalamus, a structure that combines photic and nonphotic information to regulate circadian behaviors (Morin et al. 2003; Hattar et al. 2006; Fernandez et al. 2020; Beier et al. 2021). This targeting requires the glycoprotein Reelin in the extracellular matrix of vLGN and IGL and the intracellular signaling molecule disabled-1 (Dab1) in M1 ipRGCs (Su et al. 2011). Dab1

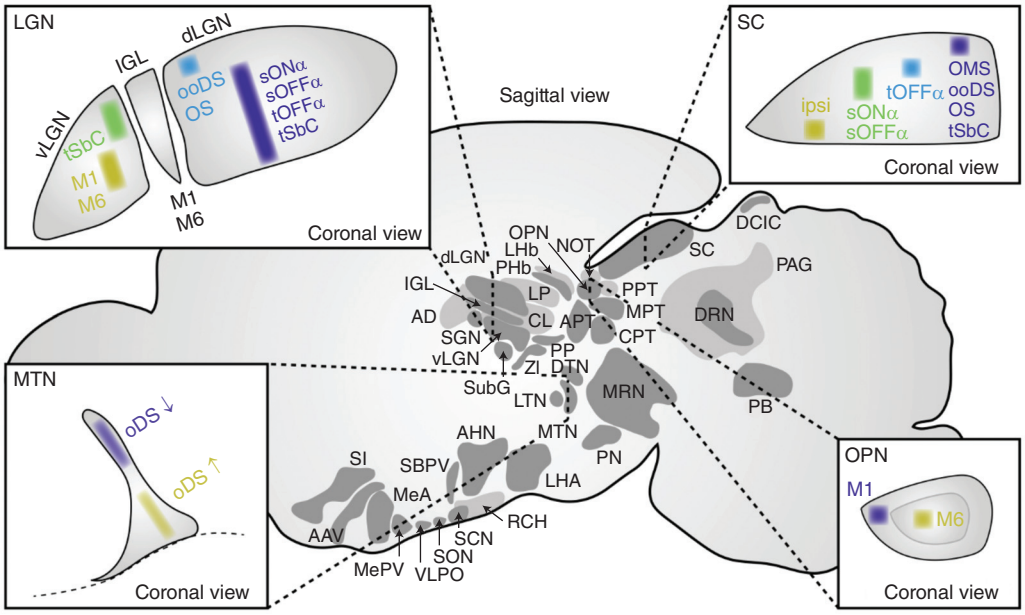


**Figure 2.** Retinorecipient brain targets and retinal ganglion cell (RGC)-type-specific lamination. Background illustration of the distribution of retinorecipient targets in a sagittal view of the mouse brain. (SI) Substantia innominata, (AAV) ventral anterior amygdaloid area, (MeA) anterior medial amygdala, (MePV) posteroventral medial amygdala, (VLPO) ventrolateral preoptic area, (SON) supraoptic nucleus, (SCN) suprachiasmatic nucleus, (RCH) retrochiasmatic area, (SBPV) subparaventricular zone, (AHN) anterior hypothalamic area, (LHN) lateral hypothalamic area, (PN) paranigral nucleus, (MRN) midbrain reticular nucleus, (MTN) medial terminal nucleus, (LTN) lateral terminal nucleus, (DTN) dorsal terminal nucleus, (ZI) zona incerta, (PP) peripeduncular nucleus, (SubG) subgeniculate nucleus, (vLGN) ventrolateral geniculate nucleus, (SGN) suprageniculate nucleus, (AD) anterodorsal thalamic nucleus, (IGL) intergeniculate leaflet, (CL) centrolateral thalamic nucleus, (dLGN) dorsolateral geniculate nucleus of the thalamus, (LP) lateral posterior nucleus of the thalamus, (APT) anterior pretectal nucleus, (CPT) commissural pretectal nucleus, (MPT) medial pretectal nucleus, (PPT) posterior pretectal nucleus, (PHb) perihabenular nucleus, (LHb) lateral habenula, (OPN) olivary pretectal nucleus, (NOT) nucleus of the optic tract, (SC) superior colliculus, (DCIC) dorsal cortex of the inferior colliculus, (PAG) periaqueductal gray, (DRN) dorsal raphe nucleus, (PB) parabrachial nucleus, (tSbC) transient suppressed-by-contrast. *Insets* in the foreground show the RGC-type-specific lamination of RGC axons in the LGN complex (*top left*), SC (*top right*), MTN (*bottom left*), and OPN (*bottom right*) in coronal views. (oDS) ON DS RGCs, (ooDS) ON-OFF DS RGCs.

mediates Reelin signals transmitted via VLDLR and ApoER2 receptors on the M1 ipRGC axons (Su et al. 2011).

The M6 ipRGC targeting of pretectal nuclei (i.e., OPN and the medial division of the posterior pretectal nucleus or mdPPN) depends on the matching expression of the homophilically interacting cell-adhesion molecule Cadherin-6 on the RGC axons and their postsynaptic partners (Osterhout et al. 2011). In the OPN, M6 ipRGCs target the core region (Quattrochi et al. 2019), whereas M1 ipRGCs innervate the OPN shell (Fig. 2; Chen et al. 2011). The function of this M6 ipRGC projection remains unknown.

Different ON DS RGC types innervate different nuclei of the accessory optic system (i.e., MTN, DTN, and NOT) to mediate horizontal and vertical gaze-stabilizing eye movements (Fig. 2; Simpson 1984). Interactions between the cell-adhesion molecule Contactin-4 on RGC axons and the amyloid precursor protein (APP) on target neurons drive the innervation of the NOT (Osterhout et al. 2015). Conversely, interactions between Semaphorin6A on RGC axons and PlexinA2/A4 on target neurons mediate ON DS RGC targeting of the MTN and DTN (Sun et al. 2015).

## CONCLUDING REMARKS

The last 5 years represent significant progress toward a complete taxonomy of RGC types and retinorecipient brain areas in mice. This progress has opened the door for identifying the wide variety of molecular- and activity-based mechanisms that govern retina-to-brain mapping. Understanding the developmental mechanisms and sequence of retinal innervation will, in turn, advance our understanding of the adult organization of visual brain areas and how they mediate their diverse functions.

## REFERENCES

Ackman JB, Crair MC. 2014. Role of emergent neural activity in visual map development. *Curr Opin Neurobiol* **24:** 166–175. doi:10.1016/j.conb.2013.11.011

Ackman JB, Burbridge TJ, Crair MC. 2012. Retinal waves coordinate patterned activity throughout the developing visual system. *Nature* **490:** 219–225. doi:10.1038/nature11529

Ahmadlou M, Heimel JA. 2015. Preference for concentric orientations in the mouse superior colliculus. *Nat Commun* **6:** 6773. doi:10.1038/ncomms7773

Akrouh A, Kerschensteiner D. 2013. Intersecting circuits generate precisely patterned retinal waves. *Neuron* **79:** 322–334. doi:10.1016/j.neuron.2013.05.012

Assali A, Gaspar P, Rebsam A. 2014. Activity dependent mechanisms of visual map formation—from retinal waves to molecular regulators. *Semin Cell Dev Biol* **35:** 136–146. doi:10.1016/j.semcdb.2014.08.008

Badea TC, Nathans J. 2011. Morphologies of mouse retinal ganglion cells expressing transcription factors Brn3a, Brn3b, and Brn3c: analysis of wild type and mutant cells using genetically-directed sparse labeling. *Vision Res* **51:** 269–279. doi:10.1016/j.visres.2010.08.039

Baden T, Berens P, Franke K, Román Rosón M, Bethge M, Euler T. 2016. The functional diversity of retinal ganglion cells in the mouse. *Nature* **529:** 345–350. doi:10.1038/nature16468

Baden T, Euler T, Berens P. 2020. Understanding the retinal basis of vision across species. *Nat Rev Neurosci* **21:** 5–20. doi:10.1038/s41583-019-0242-1

Bae JA, Mu S, Kim JS, Turner NL, Tartavull I, Kemnitz N, Jordan CS, Norton AD, Silversmith WM, Prentki R, et al. 2018. Digital museum of retinal ganglion cells with dense anatomy and physiology. *Cell* **173:** 1293–1306.e19. doi:10.1016/j.cell.2018.04.040

Bakken TE, van Velthoven CT, Menon V, Hodge RD, Yao Z, Nguyen TN, Graybuck LT, Horwitz GD, Bertagnolli D, Goldy J, et al. 2021. Single-cell and single-nucleus RNA-seq uncovers shared and distinct axes of variation in dorsal LGN neurons in mice, non-human primates, and humans. *eLife* **10:** e64875. doi:10.7554/eLife.64875

Bansal A, Singer JH, Hwang BJ, Xu W, Beaudet A, Feller MB. 2000. Mice lacking specific nicotinic acetylcholine receptor subunits exhibit dramatically altered spontaneous activity patterns and reveal a limited role for retinal waves in forming ON and OFF circuits in the inner retina. *J Neurosci* **20:** 7672–7681. doi:10.1523/JNEUROSCI.20-20-07672.2000

Bauer J, Weiler S, Fernholz MHP, Laubender D, Scheuss V, Hübener M, Bonhoeffer T, Rose T. 2021. Limited functional convergence of eye-specific inputs in the retinogeniculate pathway of the mouse. *Neuron* **109:** 2457–2468.e12. doi:10.1016/j.neuron.2021.05.036

Baver SB, Pickard GE, Sollars PJ, Pickard GE. 2008. Two types of melanopsin retinal ganglion cell differentially innervate the hypothalamic suprachiasmatic nucleus and the olivary pretectal nucleus. *Eur J Neurosci* **27:** 1763–1770. doi:10.1111/j.1460-9568.2008.06149.x

Beier C, Zhang Z, Yurgel M, Hattar S. 2021. Projections of ipRGCs and conventional RGCs to retinorecipient brain nuclei. *J Comp Neurol* **529:** 1863–1875. doi:10.1002/cne.25061

Benjumeda I, Escalante A, Law C, Morales D, Chauvin G, Muça G, Coca Y, Márquez J, López-Bendito G, Kania A, et al. 2013. Uncoupling of EphA/ephrinA signaling and spontaneous activity in neural circuit wiring. *J Neurosci* **33:** 18208–18218. doi:10.1523/JNEUROSCI.1931-13.2013

Berry MH, Moldavan M, Garrett T, Meadows M, Cravetchi O, White E, Leffler J, von Gersdorff H, Wright KM, Allen CN, et al. 2023. A melanopsin ganglion cell subtype forms a dorsal retinal mosaic projecting to the supraoptic nucleus. *Nat Commun* **14:** 1492.

Bleckert A, Schwartz GW, Turner MH, Rieke F, Wong ROL. 2014. Visual space is represented by nonmatching topographies of distinct mouse retinal ganglion cell types. *Curr Biol* **24:** 310–315. doi:10.1016/j.cub.2013.12.020

Burbridge TJ, Xu HP, Ackman JB, Ge X, Zhang Y, Ye MJ, Zhou ZJ, Xu J, Contractor A, Crair MC. 2014. Visual circuit development requires patterned activity mediated by retinal acetylcholine receptors. *Neuron* **84:** 1049–1064. doi:10.1016/j.neuron.2014.10.051

Butts DA, Kanold PO, Shatz CJ. 2007. A burst-based "Hebbian" learning rule at retinogeniculate synapses links retinal waves to activity-dependent refinement. *PLoS Biol* **5:** e61. doi:10.1371/journal.pbio.0050061

Cang J, Feldheim DA. 2013. Developmental mechanisms of topographic map formation and alignment. *Annu Rev Neurosci* **36:** 51–77. doi:10.1146/annurev-neuro-062012-170341

Cang J, Wang L, Stryker MP, Feldheim DA. 2008. Roles of ephrin-as and structured activity in the development of functional maps in the superior colliculus. *J Neurosci* **28:** 11015–11023. doi:10.1523/JNEUROSCI.2478-08.2008

Cang J, Savier E, Barchini J, Liu X. 2018. Visual function, organization, and development of the mouse superior colliculus. *Annu Rev Vis Sci* **4:** 239–262. doi:10.1146/annurev-vision-091517-034142

Catsicas M, Bonness V, Becker D, Mobbs P. 1998. Spontaneous $Ca^{2+}$ transients and their transmission in the developing chick retina. *Curr Biol* **8:** 283–286. doi:10.1016/S0960-9822(98)70110-1

Caval-Holme FS, Aranda ML, Chen AQ, Tiriac A, Zhang Y, Smith B, Birnbaumer L, Schmidt TM, Feller MB. 2022. The retinal basis of light aversion in neonatal mice. *J Neurosci* **42:** 4101–4115. doi:10.1523/JNEUROSCI.0151-22.2022

Chandrasekaran AR, Plas DT, Gonzalez E, Crair MC. 2005. Evidence for an instructive role of retinal activity in retinotopic map refinement in the superior colliculus of the mouse. *J Neurosci* **25:** 6929–6938. doi:10.1523/JNEUROSCI.1470-05.2005

Chandrasekaran AR, Shah RD, Crair MC. 2007. Developmental homeostasis of mouse retinocollicular synapses. *J Neurosci* **27:** 1746–1755. doi:10.1523/JNEUROSCI.4383-06.2007

Chen C, Regehr WG. 2000. Developmental remodeling of the retinogeniculate synapse. *Neuron* **28:** 955–966. doi:10.1016/S0896-6273(00)00166-5

Chen S-K, Badea TC, Hattar S. 2011. Photoentrainment and pupillary light reflex are mediated by distinct populations of ipRGCs. *Nature* **476:** 92–95. doi:10.1038/nature10206

Chen H, Savier EL, DePiero VJ, Cang J. 2021. Lack of evidence for stereotypical direction columns in the mouse superior colliculus. *J Neurosci* **41:** 461–473. doi:10.1523/JNEUROSCI.1155-20.2020

Cheng HJ, Nakamoto M, Bergemann AD, Flanagan JG. 1995. Complementary gradients in expression and binding of ELF-1 and Mek4 in development of the topographic retinotectal projection map. *Cell* **82:** 371–381. doi:10.1016/0092-8674(95)90426-3

Cramer KS, Sur M. 1997. Blockade of afferent impulse activity disrupts on/off sublamination in the ferret lateral geniculate nucleus. *Brain Res Dev Brain Res* **98:** 287–290. doi:10.1016/S0165-3806(96)00188-5

Cruz-Martín A, El-Danaf RN, Osakada F, Sriram B, Dhande OS, Nguyen PL, Callaway EM, Ghosh A, Huberman AD. 2014. A dedicated circuit links direction-selective retinal ganglion cells to the primary visual cortex. *Nature* **507:** 358–361. doi:10.1038/nature12989

Dacey DM. 2004. Origins of perception: retinal ganglion cell diversity and the creation of parallel visual pathways. *Cogn Neurosci* **3:** 281–301.

Dai J, Buhusi M, Demyanenko GP, Brennaman LH, Hruska M, Dalva MB, Maness PF. 2013. Neuron glia-related cell adhesion molecule (NrCAM) promotes topographic retinocollicular mapping. *PLoS ONE* **8:** e73000. doi:10.1371/journal.pone.0073000

de Malmazet D, Kühn NK, Farrow K. 2018. Retinotopic separation of nasal and temporal motion selectivity in the mouse superior colliculus. *Curr Biol* **28:** 2961–2969.e4. doi:10.1016/j.cub.2018.07.001

Demas J, Eglen SJ, Wong ROL. 2003. Developmental loss of synchronous spontaneous activity in the mouse retina is independent of visual experience. *J Neurosci* **23:** 2851–2860. doi:10.1523/JNEUROSCI.23-07-02851.2003

Demas J, Sagdullaev BT, Green E, Jaubert-Miazza L, McCall MA, Gregg RG, Wong ROL, Guido W. 2006. Failure to maintain eye-specific segregation in nob, a mutant with abnormally patterned retinal activity. *Neuron* **50:** 247–259. doi:10.1016/j.neuron.2006.03.033

Dhande OS, Hua EW, Guh E, Yeh J, Bhatt S, Zhang Y, Ruthazer ES, Feller MB, Crair MC. 2011. Development of single retinofugal axon arbors in normal and β2 knockout mice. *J Neurosci* **31:** 3384–3399. doi:10.1523/JNEUROSCI.4899-10.2011

Dhande OS, Stafford BK, Lim JHA, Huberman AD. 2015. Contributions of retinal ganglion cells to subcortical visual processing and behaviors. *Annu Rev Vis Sci* **1:** 291–328. doi:10.1146/annurev-vision-082114-035502

Dimitrov D, Türei D, Garrido-Rodriguez M, Burmedi PL, Nagai JS, Boys C, Ramirez Flores RO, Kim H, Szalai B, Costa IG, et al. 2022. Comparison of methods and resources for cell-cell communication inference from single-cell RNA-seq data. *Nat Commun* **13:** 3224. doi:10.1038/s41467-022-30755-0

Dräger UC, Hubel DH. 1976. Topography of visual and somatosensory projections to mouse superior colliculus. *J Neurophysiol* **39:** 91–101. doi:10.1152/jn.1976.39.1.91

Dräger UC, Olsen JF. 1980. Origins of crossed and uncrossed retinal projections in pigmented and albino mice. *J Comp Neurol* **191:** 383–412. doi:10.1002/cne.901910306

Dräger UC, Olsen JF. 1981. Ganglion cell distribution in the retina of the mouse. *Invest Ophthalmol Vis Sci* **20:** 285–293.

Ecker JL, Dumitrescu ON, Wong KY, Alam NM, Chen SK, LeGates T, Renna JM, Prusky GT, Berson DM, Hattar S. 2010. Melanopsin-expressing retinal ganglion-cell photoreceptors: cellular diversity and role in pattern vision. *Neuron* **67:** 49–60. doi:10.1016/j.neuron.2010.05.023

El-Danaf RN, Huberman AD. 2019. Sub-topographic maps for regionally enhanced analysis of visual space in the mouse retina. *J Comp Neurol* **527:** 259–269. doi:10.1002/cne.24457

Ellis EM, Gauvain G, Sivyer B, Murphy GJ. 2016. Shared and distinct retinal input to the mouse superior colliculus and dorsal lateral geniculate nucleus. *J Neurophysiol* **116:** 602–610. doi:10.1152/jn.00227.2016

Elstrott J, Feller MB. 2010. Direction-selective ganglion cells show symmetric participation in retinal waves during development. *J Neurosci* **30:** 11197–11201. doi:10.1523/JNEUROSCI.2302-10.2010

Erskine L, Reijntjes S, Pratt T, Denti L, Schwarz Q, Vieira JM, Alakakone B, Shewan D, Ruhrberg C. 2011. VEGF signaling through neuropilin 1 guides commissural axon crossing at the optic chiasm. *Neuron* **70:** 951–965. doi:10.1016/j.neuron.2011.02.052

Fabre PJ, Shimogori T, Charron F. 2010. Segregation of ipsilateral retinal ganglion cell axons at the optic chiasm requires the Shh receptor Boc. *J Neurosci* **30:** 266–275. doi:10.1523/JNEUROSCI.3778-09.2010

Feinberg EH, Meister M. 2015. Orientation columns in the mouse superior colliculus. *Nature* **519:** 229–232. doi:10.1038/nature14103

Feldheim DA, Vanderhaeghen P, Hansen MJ, Frisén J, Lu Q, Barbacid M, Flanagan JG. 1998. Topographic guidance labels in a sensory projection to the forebrain. *Neuron* **21:** 1303–1313. doi:10.1016/S0896-6273(00)80650-9

Feldheim DA, Kim YI, Bergemann AD, Frisén J, Barbacid M, Flanagan JG. 2000. Genetic analysis of ephrin-A2 and ephrin-A5 shows their requirement in multiple aspects of retinocollicular mapping. *Neuron* **25:** 563–574. doi:10.1016/S0896-6273(00)81060-0

Fernandez DC, Chang YT, Hattar S, Chen SK. 2016. Architecture of retinal projections to the central circadian pacemaker. *Proc Natl Acad Sci* **113:** 6047–6052. doi:10.1073/pnas.1523629113

Fernandez DC, Komal R, Langel J, Ma J, Duy PQ, Penzo MA, Zhao H, Hattar S. 2020. Retinal innervation tunes circuits that drive nonphotic entrainment to food. *Nature* **581:** 194–198. doi:10.1038/s41586-020-2204-1

Fisher LJ. 1979. Development of synaptic arrays in the inner plexiform layer of neonatal mouse retina. *J Comp Neurol* **187:** 359–372. doi:10.1002/cne.901870207

Ford KJ, Félix AL, Feller MB. 2012. Cellular mechanisms underlying spatiotemporal features of cholinergic retinal waves. *J Neurosci* **32:** 850–863. doi:10.1523/JNEUROSCI.5309-12.2012

Fratzl A, Koltchev AM, Vissers N, Tan YL, Marques-Smith A, Stempel AV, Branco T, Hofer SB. 2021. Flexible inhibitory control of visually evoked defensive behavior by the ventral lateral geniculate nucleus. *Neuron* **109:** 3810–3822.e9. doi:10.1016/j.neuron.2021.09.003

Frisén J, Yates PA, McLaughlin T, Friedman GC, O'Leary DD, Barbacid M. 1998. Ephrin-A5 (AL-1/RAGS) is essential for proper retinal axon guidance and topographic mapping in the mammalian visual system. *Neuron* **20:** 235–243. doi:10.1016/S0896-6273(00)80452-3

Fukuda Y, Sawai H, Watanabe M, Wakakuwa K, Morigiwa K. 1989. Nasotemporal overlap of crossed and uncrossed retinal ganglion cell projections in the Japanese monkey (*Macaca fuscata*). *J Neurosci* **9:** 2353–2373. doi:10.1523/JNEUROSCI.09-07-02353.1989

Gale SD, Murphy GJ. 2014. Distinct representation and distribution of visual information by specific cell types in mouse superficial superior colliculus. *J Neurosci* **34:** 13458–13471. doi:10.1523/JNEUROSCI.2768-14.2014

García-Frigola C, Herrera E. 2010. Zic2 regulates the expression of Sert to modulate eye-specific refinement at the visual targets. *EMBO J* **29:** 3170–3183. doi:10.1038/emboj.2010.172

García-Frigola C, Carreres MI, Vegar C, Mason C, Herrera E. 2008. Zic2 promotes axonal divergence at the optic chiasm midline by EphB1-dependent and -independent mechanisms. *Development* **135:** 1833–1841. doi:10.1242/dev.020693

Gauvain G, Murphy GJ. 2015. Projection-specific characteristics of retinal input to the brain. *J Neurosci* **35:** 6575–6583. doi:10.1523/JNEUROSCI.4298-14.2015

Ge X, Zhang K, Gribizis A, Hamodi AS, Sabino AM, Crair MC. 2021. Retinal waves prime visual motion detection by simulating future optic flow. *Science* **373:** eabd0830. doi:10.1126/science.abd0830

Gjorgjieva J, Toyoizumi T, Eglen SJ. 2009. Burst-time-dependent plasticity robustly guides ON/OFF segregation in the lateral geniculate nucleus. *PLoS Comput Biol* **5:** e1000618. doi:10.1371/journal.pcbi.1000618

Godement P, Salaün J, Imbert M. 1984. Prenatal and postnatal development of retinogeniculate and retinocollicular projections in the mouse. *J Comp Neurol* **230:** 552–575. doi:10.1002/cne.902300406

Goetz J, Jessen ZF, Jacobi A, Mani A, Cooler S, Greer D, Kadri S, Segal J, Shekhar K, Sanes JR, et al. 2022. Unified classification of mouse retinal ganglion cells using function, morphology, and gene expression. *Cell Rep* **40:** 111040. doi:10.1016/j.celrep.2022.111040

Gribizis A, Ge X, Daigle TL, Ackman JB, Zeng H, Lee D, Crair MC. 2019. Visual cortex gains independence from peripheral drive before eye opening. *Neuron* **104:** 711–723.e3. doi:10.1016/j.neuron.2019.08.015

Grubb MS, Rossi FM, Changeux JP, Thompson ID. 2003. Abnormal functional organization in the dorsal lateral geniculate nucleus of mice lacking the β2 subunit of the nicotinic acetylcholine receptor. *Neuron* **40:** 1161–1172. doi:10.1016/S0896-6273(03)00789-X

Güler AD, Ecker JL, Lall GS, Haq S, Altimus CM, Liao H-W, Barnard AR, Cahill H, Badea TC, Zhao H, et al. 2008. Melanopsin cells are the principal conduits for rod-cone input to non-image-forming vision. *Nature* **453:** 102–105. doi:10.1038/nature06829

Gupta D, Młynarski W, Sumser A, Symonova O, Svatoň J, Joesch M. 2023. Panoramic visual statistics shape retina-wide organization of receptive fields. *Nat Neurosci* **26:** 606–614. doi:10.1038/s41593-023-01280-0

Hahm JO, Langdon RB, Sur M. 1991. Disruption of retinogeniculate afferent segregation by antagonists to NMDA receptors. *Nature* **351:** 568–570. doi:10.1038/351568a0

Hammer S, Monavarfeshani A, Lemon T, Su J, Fox MA. 2015. Multiple retinal axons converge onto relay cells in the adult mouse thalamus. *Cell Rep* **12:** 1575–1583. doi:10.1016/j.celrep.2015.08.003

Hasse JM, Briggs F. 2017. A cross-species comparison of corticogeniculate structure and function. *Vis Neurosci* **34:** E016. doi:10.1017/S095252381700013X

Hattar S, Kumar M, Park A, Tong P, Tung J, Yau KW, Berson DM. 2006. Central projections of melanopsin-expressing retinal ganglion cells in the mouse. *J Comp Neurol* **497:** 326–349. doi:10.1002/cne.20970

Haustead DJ, Lukehurst SS, Clutton GT, Bartlett CA, Dunlop SA, Arrese CA, Sherrard RM, Rodger J. 2008. Functional topography and integration of the contralateral and ipsilateral retinocollicular projections of *ephrin-A*$^{-/-}$ mice. *J Neurosci* **28:** 7376–7386. doi:10.1523/JNEUROSCI.1135-08.2008

Hendrickson A, Wilson ME, Toyne MJ. 1970. The distribution of optic nerve fibers in *Macaca mulatta*. *Brain Res* **23:** 425–427. doi:10.1016/0006-8993(70)90068-5

Herrera E, Brown L, Aruga J, Rachel RA, Dolen G, Mikoshiba K, Brown S, Mason CA. 2003. Zic2 patterns binocular vision by specifying the uncrossed retinal projection. *Cell* **114:** 545–557. doi:10.1016/S0092-8674(03)00684-6

Heukamp AS, Warwick RA, Rivlin-Etzion M. 2020. Topographic variations in retinal encoding of visual space. *Annu Rev Vis Sci* **6:** 237–259. doi:10.1146/annurev-vision-121219-081831

Hindges R, McLaughlin T, Genoud N, Henkemeyer M, O'Leary DDM. 2002. Ephb forward signaling controls directional branch extension and arborization required for dorsal-ventral retinotopic mapping. *Neuron* **35:** 475–487. doi:10.1016/S0896-6273(02)00799-7

Holcombe V, Guillery RW. 1984. The organization of retinal maps within the dorsal and ventral lateral geniculate nuclei of the rabbit. *J Comp Neurol* **225:** 469–491. doi:10.1002/cne.902250402

Hong YK, Kim IJ, Sanes JR. 2011. Stereotyped axonal arbors of retinal ganglion cell subsets in the mouse superior colliculus. *J Comp Neurol* **519:** 1691–1711. doi:10.1002/cne.22595

Hong YK, Park S, Litvina EY, Morales J, Sanes JR, Chen C. 2014. Refinement of the retinogeniculate synapse by bouton clustering. *Neuron* **84:** 332–339. doi:10.1016/j.neuron.2014.08.059

Hong YK, Burr EF, Sanes JR, Chen C. 2019. Heterogeneity of retinogeniculate axon arbors. *Eur J Neurosci* **49:** 948–956. doi:10.1111/ejn.13986

Hooks BM, Chen C. 2006. Distinct roles for spontaneous and visual activity in remodeling of the retinogeniculate synapse. *Neuron* **52:** 281–291. doi:10.1016/j.neuron.2006.07.007

Hooks BM, Chen C. 2008. Vision triggers an experience-dependent sensitive period at the retinogeniculate synapse. *J Neurosci* **28:** 4807–4817. doi:10.1523/JNEUROSCI.4667-07.2008

Howarth M, Walmsley L, Brown TM. 2014. Binocular integration in the mouse lateral geniculate nuclei. *Curr Biol* **24:** 1241–1247. doi:10.1016/j.cub.2014.04.014

Hoy JL, Bishop HI, Niell CM. 2019. Defined cell types in superior colliculus make distinct contributions to prey capture behavior in the mouse. *Curr Biol* **29:** 4130–4138.e5. doi:10.1016/j.cub.2019.10.017

Hu Z, Mu Y, Huang L, Hu Y, Chen Z, Yang Y, Huang X, Fu Y, Xi Y, Lin S, et al. 2022. A visual circuit related to the periaqueductal gray area for the antinociceptive effects of bright light treatment. *Neuron* **110:** 1712–1727.e7. doi:10.1016/j.neuron.2022.02.009

Huang L, Xi Y, Peng Y, Yang Y, Huang X, Fu Y, Tao Q, Xiao J, Yuan T, An K, et al. 2019. A visual circuit related to habenula underlies the antidepressive effects of light therapy. *Neuron* **102:** 128–142.e8. doi:10.1016/j.neuron.2019.01.037

Huang X, Huang P, Huang L, Hu Z, Liu X, Shen J, Xi Y, Yang Y, Fu Y, Tao Q, et al. 2021. A visual circuit related to the nucleus reuniens for the spatial-memory-promoting effects of light treatment. *Neuron* **109:** 347–362.e7. doi:10.1016/j.neuron.2020.10.023

Huang W, Xu Q, Su J, Tang L, Hao ZZ, Xu C, Liu R, Shen Y, Sang X, Xu N, et al. 2022. Linking transcriptomes with morphological and functional phenotypes in mammalian retinal ganglion cells. *Cell Rep* **40:** 111322. doi:10.1016/j.celrep.2022.111322

Huang YF, Liao PY, Yu JH, Chen SK. 2023. Light disrupts social memory via a retina-to-supraoptic nucleus circuit. *EMBO Rep* **2023:** e56839. doi:10.15252/embr.202356839

Huberman AD, Murray KD, Warland DK, Feldheim DA, Chapman B. 2005. Ephrin-As mediate targeting of eye-specific projections to the lateral geniculate nucleus. *Nat Neurosci* **8:** 1013–1021. doi:10.1038/nn1505

Huberman AD, Manu M, Koch SM, Susman MW, Lutz AB, Ullian EM, Baccus SA, Barres BA. 2008. Architecture and activity-mediated refinement of axonal projections from a mosaic of genetically identified retinal ganglion cells. *Neuron* **59:** 425–438. doi:10.1016/j.neuron.2008.07.018

Huberman AD, Wei W, Elstrott J, Stafford BK, Feller MB, Barres BA. 2009. Genetic identification of an on-off direction-selective retinal ganglion cell subtype reveals a layer-specific subcortical map of posterior motion. *Neuron* **62:** 327–334. doi:10.1016/j.neuron.2009.04.014

Illing RB, Wässle H. 1981. The retinal projection to the thalamus in the cat: a quantitative investigation and a comparison with the retinotectal pathway. *J Comp Neurol* **202:** 265–285. doi:10.1002/cne.902020211

Ivanova E, Hwang GS, Pan ZH. 2010. Characterization of transgenic mouse lines expressing Cre recombinase in the retina. *Neuroscience* **165:** 233–243. doi:10.1016/j.neuroscience.2009.10.021

Johnson KO, Triplett JW. 2021. Wiring subcortical image-forming centers: topography, laminar targeting, and map alignment. *Curr Top Dev Biol* **142:** 283–317. doi:10.1016/bs.ctdb.2020.10.004

Johnson KP, Zhao L, Kerschensteiner D. 2018. A pixel-encoder retinal ganglion cell with spatially offset excitatory and inhibitory receptive fields. *Cell Rep* **22:** 1462–1472. doi:10.1016/j.celrep.2018.01.037

Johnson KP, Fitzpatrick MJ, Zhao L, Wang B, McCracken S, Williams PR, Kerschensteiner D. 2021. Cell-type-specific binocular vision guides predation in mice. *Neuron* **109:** 1527–1539.e4. doi:10.1016/j.neuron.2021.03.010

Johnson KO, Harel L, Triplett JW. 2023. Postsynaptic NMDA receptor expression is required for visual cortico-collicular projection refinement in the mouse superior colliculus. *J Neurosci* **43:** 1310–1320. doi:10.1523/JNEUROSCI.1473-22.2022

Kay JN, De la Huerta I, Kim I-J, Zhang Y, Yamagata M, Chu MW, Meister M, Sanes JR. 2011. Retinal ganglion cells

with distinct directional preferences differ in molecular identity, structure, and central projections. *J Neurosci* **31:** 7753–7762. doi:10.1523/JNEUROSCI.0907-11.2011

Kerschensteiner D. 2016. Glutamatergic retinal waves. *Front Neural Circuits* **10:** 38. doi:10.3389/fncir.2016.00038

Kerschensteiner D. 2020. Mammalian retina development. In *The senses: a comprehensive reference*, 2nd ed (ed. Fritzsch B), pp. 234–251. Elsevier, Oxford.

Kerschensteiner D. 2022. Feature detection by retinal ganglion cells. *Annu Rev Vis Sci* **8:** 135–169. doi:10.1146/annurev-vision-100419-112009

Kerschensteiner D, Guido W. 2017. Organization of the dorsal lateral geniculate nucleus in the mouse. *Vis Neurosci* **34:** E008. doi:10.1017/S0952523817000062

Kerschensteiner D, Wong ROL. 2008. A precisely timed asynchronous pattern of ON and OFF retinal ganglion cell activity during propagation of retinal waves. *Neuron* **58:** 851–858. doi:10.1016/j.neuron.2008.04.025

Kim IJ, Zhang Y, Yamagata M, Meister M, Sanes JR. 2008. Molecular identification of a retinal cell type that responds to upward motion. *Nature* **452:** 478–482. doi:10.1038/nature06739

Kim I-J, Zhang Y, Meister M, Sanes JR. 2010. Laminar restriction of retinal ganglion cell dendrites and axons: subtype-specific developmental patterns revealed with transgenic markers. *J Neurosci* **30:** 1452–1462. doi:10.1523/JNEUROSCI.4779-09.2010

Kim T, Shen N, Hsiang JC, Johnson KP, Kerschensteiner D. 2020. Dendritic and parallel processing of visual threats in the retina control defensive responses. *Sci Adv* **6:** eabc9920. doi:10.1126/sciadv.abc9920

Kirkby LA, Sack GS, Firl A, Feller MB. 2014. Erratum to: A role for correlated spontaneous activity in the assembly of neural circuits [Neuron 80 (2013) 1129–1144]. *Neuron* **81:** 218. doi:10.1016/j.neuron.2013.12.031

Knudsen EI, Brainard MS. 1995. Creating a unified representation of visual and auditory space in the brain. *Annu Rev Neurosci* **18:** 19–43. doi:10.1146/annurev.ne.18.030195.000315

Koch SM, Ullian EM. 2010. Neuronal pentraxins mediate silent synapse conversion in the developing visual system. *J Neurosci* **30:** 5404–5414. doi:10.1523/JNEUROSCI.4893-09.2010

Koch SM, Dela Cruz CG, Hnasko TS, Edwards RH, Huberman AD, Ullian EM. 2011. Pathway-specific genetic attenuation of glutamate release alters select features of competition-based visual circuit refinement. *Neuron* **71:** 235–242. doi:10.1016/j.neuron.2011.05.045

Krahe TE, El-Danaf RN, Dilger EK, Henderson SC, Guido W. 2011. Morphologically distinct classes of relay cells exhibit regional preferences in the dorsal lateral geniculate nucleus of the mouse. *J Neurosci* **31:** 17437–17448. doi:10.1523/jneurosci.4370-11.2011

Kruijt CC, de Wit GC, Bergen AA, Florijn RJ, Schalij-Delfos NE, van Genderen MM. 2018. The phenotypic spectrum of albinism. *Ophthalmology* **125:** 1953–1960. doi:10.1016/j.ophtha.2018.08.003

Kuwajima T, Yoshida Y, Takegahara N, Petros TJ, Kumanogoh A, Jessell TM, Sakurai T, Mason C. 2012. Optic chiasm presentation of Semaphorin6D in the context of Plexin-A1 and Nr-CAM promotes retinal axon midline crossing. *Neuron* **74:** 676–690. doi:10.1016/j.neuron.2012.03.025

Leamey CA, Merlin S, Lattouf P, Sawatari A, Zhou X, Demel N, Glendining KA, Oohashi T, Sur M, Fässler R. 2007. Ten_m3 regulates eye-specific patterning in the mammalian visual pathway and is required for binocular vision. *PLoS Biol* **5:** e241. doi:10.1371/journal.pbio.0050241

Lee R, Petros TJ, Mason CA. 2008. Zic2 regulates retinal ganglion cell axon avoidance of ephrinB2 through inducing expression of the guidance receptor EphB1. *J Neurosci* **28:** 5910–5919. doi:10.1523/JNEUROSCI.0632-08.2008

Levine JN, Schwartz GW. 2020. The olivary pretectal nucleus receives visual input of high spatial resolution. bioRxiv doi:10.1101/2020.06.23.168054

Li YT, Meister M. 2023. Functional cell types in the mouse superior colliculus. *eLife* **12:** e82367. doi:10.7554/eLife.82367

Li YT, Turan Z, Meister M. 2020. Functional architecture of motion direction in the mouse superior colliculus. *Curr Biol* **30:** 3304–3315.e4. doi:10.1016/j.cub.2020.06.023

Liang L, Chen C. 2020. Organization, function, and development of the mouse retinogeniculate synapse. *Annu Rev Vis Sci* **6:** 261–285. doi:10.1146/annurev-vision-121219-081753

Liang F, Xiong XR, Zingg B, Ji XY, Zhang LI, Tao HW. 2015. Sensory cortical control of a visually induced arrest behavior via corticotectal projections. *Neuron* **86:** 755–767. doi:10.1016/j.neuron.2015.03.048

Liang L, Fratzl A, Goldey G, Ramesh RN, Sugden AU, Morgan JL, Chen C, Andermann ML. 2018. A fine-scale functional logic to convergence from retina to thalamus. *Cell* **173:** 1343–1355.e24. doi:10.1016/j.cell.2018.04.041

Litvina EY, Chen C. 2017. Functional convergence at the retinogeniculate synapse. *Neuron* **96:** 330–338.e5. doi:10.1016/j.neuron.2017.09.037

Liu A, Milner ES, Peng YR, Blume HA, Brown MC, Bryman GS, Emanuel AJ, Morquette P, Viet NM, Sanes JR, et al. 2023a. Encoding of environmental illumination by primate melanopsin neurons. *Science* **379:** 376–381. doi:10.1126/science.ade2024

Liu Y, Savier EL, DePiero VJ, Chen C, Schwalbe DC, Abraham-Fan RJ, Chen H, Campbell JN, Cang J. 2023b. Mapping visual functions onto molecular cell types in the mouse superior colliculus. *Neuron* **111:** 1876–1886.e5. doi:10.1016/j.neuron.2023.03.036

Lund RD, Lund JS, Wise RP. 1974. The organization of the retinal projection to the dorsal lateral geniculate nucleus in pigmented and albino rats. *J Comp Neurol* **158:** 383–403. doi:10.1002/cne.901580403

Magnin M, Cooper HM, Mick G. 1989. Retinohypothalamic pathway: a breach in the law of Newton-Müller-Gudden? *Brain Res* **488:** 390–397. doi:10.1016/0006-8993(89)90737-3

Maiorano NA, Hindges R. 2013. Restricted perinatal retinal degeneration induces retina reshaping and correlated structural rearrangement of the retinotopic map. *Nat Commun* **4:** 1938. doi:10.1038/ncomms2926

Martersteck EM, Hirokawa KE, Evarts M, Bernard A, Duan X, Li Y, Ng L, Oh SW, Ouellette B, Royall JJ, et al. 2017. Diverse central projection patterns of retinal ganglion

Cold Spring Harbor Perspectives in Biology
www.cshperspectives.org

cells. *Cell Rep* **18:** 2058–2072. doi:10.1016/j.celrep.2017.01.075

Mason C, Slavi N. 2020. Retinal ganglion cell axon wiring establishing the binocular circuit. *Annu Rev Vis Sci* **6:** 215–236. doi:10.1146/annurev-vision-091517-034306

McLaughlin T, Torborg CL, Feller MB, O'Leary DDM. 2003. Retinotopic map refinement requires spontaneous retinal waves during a brief critical period of development. *Neuron* **40:** 1147–1160. doi:10.1016/S0896-6273(03)00790-6

McNeill DS, Sheely CJ, Ecker JL, Badea TC, Morhardt D, Guido W, Hattar S. 2011. Development of melanopsin-based irradiance detecting circuitry. *Neural Dev* **6:** 8. doi:10.1186/1749-8104-6-8

Meng JJ, Shen JW, Li G, Ouyang CJ, Hu JX, Li ZS, Zhao H, Shi YM, Zhang M, Liu R, et al. 2023. Light modulates glucose metabolism by a retina-hypothalamus-brown adipose tissue axis. *Cell* **186:** 398–412.e17. doi:10.1016/j.cell.2022.12.024

Milner ES, Do MTH. 2017. A population representation of absolute light intensity in the mammalian retina. *Cell* **171:** 865–876.e16. doi:10.1016/j.cell.2017.09.005

Monavarfeshani A, Sabbagh U, Fox MA. 2017. Not a one-trick pony: diverse connectivity and functions of the rodent lateral geniculate complex. *Vis Neurosci* **34:** E012. doi:10.1017/S0952523817000098

Monavarfeshani A, Stanton G, Van Name J, Su K, Mills WA 3rd, Swilling K, Kerr A, Huebschman NA, Su J, Fox MA. 2018. LRRTM1 underlies synaptic convergence in visual thalamus. *eLife* **7:** e33498. doi:10.7554/eLife.33498

Monosov IE, Ogasawara T, Haber SN, Heimel JA, Ahmadlou M. 2022. The zona incerta in control of novelty seeking and investigation across species. *Curr Opin Neurobiol* **77:** 102650. doi:10.1016/j.conb.2022.102650

Moreno-Juan V, Aníbal-Martínez M, Herrero-Navarro Á, Valdeolmillos M, Martini FJ, López-Bendito G. 2023. Spontaneous thalamic activity modulates the cortical innervation of the primary visual nucleus of the thalamus. *Neuroscience* **508:** 87–97. doi:10.1016/j.neuroscience.2022.07.022

Morgan JL, Lichtman JW. 2020. An individual interneuron participates in many kinds of inhibition and innervates much of the mouse visual thalamus. *Neuron* **106:** 468–481.e2. doi:10.1016/j.neuron.2020.02.001

Morgan JL, Schubert T, Wong ROL. 2008. Developmental patterning of glutamatergic synapses onto retinal ganglion cells. *Neural Dev* **3:** 8. doi:10.1186/1749-8104-3-8

Morgan JL, Berger DR, Wetzel AW, Lichtman JW. 2016. The fuzzy logic of network connectivity in mouse visual thalamus. *Cell* **165:** 192–206. doi:10.1016/j.cell.2016.02.033

Morin LP, Studholme KM. 2014. Retinofugal projections in the mouse. *J Comp Neurol* **522:** 3733–3753. doi:10.1002/cne.23635

Morin LP, Blanchard JH, Provencio I. 2003. Retinal ganglion cell projections to the hamster suprachiasmatic nucleus, intergeniculate leaflet, and visual midbrain: bifurcation and melanopsin immunoreactivity. *J Comp Neurol* **465:** 401–416. doi:10.1002/cne.10881

Mrsic-Flogel TD, Hofer SB, Creutzfeldt C, Cloëz-Tayarani I, Changeux JP, Bonhoeffer T, Hübener M. 2005. Altered map of visual space in the superior colliculus of mice lacking early retinal waves. *J Neurosci* **25:** 6921–6928. doi:10.1523/JNEUROSCI.1555-05.2005

Muellner FE, Roska B. 2023. Individual thalamic inhibitory interneurons are functionally specialized towards distinct visual features. bioRxiv doi:10.1101/2023.03.22.533751

Muir-Robinson G, Hwang BJ, Feller MB. 2002. Retinogeniculate axons undergo eye-specific segregation in the absence of eye-specific layers. *J Neurosci* **22:** 5259–5264. doi:10.1523/JNEUROSCI.22-13-05259.2002

Münch TA, da Silveira RA, Siegert S, Viney TJ, Awatramani GB, Roska B. 2009. Approach sensitivity in the retina processed by a multifunctional neural circuit. *Nat Neurosci* **12:** 1308–1316. doi:10.1038/nn.2389

Nakamoto M, Cheng HJ, Friedman GC, McLaughlin T, Hansen MJ, Yoon CH, O'Leary DD, Flanagan JG. 1996. Topographically specific effects of ELF-1 on retinal axon guidance in vitro and retinal axon mapping in vivo. *Cell* **86:** 755–766. doi:10.1016/S0092-8674(00)80150-6

Nakamoto C, Durward E, Horie M, Nakamoto M. 2019. Nell2 regulates the contralateral-versus-ipsilateral visual projection as a domain-specific positional cue. *Development* **146:** dev170704. doi:10.1242/dev.170704

Nath A, Schwartz GW. 2017. Electrical synapses convey orientation selectivity in the mouse retina. *Nat Commun* **8:** 2025. doi:10.1038/s41467-017-01980-9

O'Brien BJ, Abel PL, Olavarria JF. 2001. The retinal input to calbindin-D28k-defined subdivisions in macaque inferior pulvinar. *Neurosci Lett* **312:** 145–148. doi:10.1016/S0304-3940(01)02220-0

Osterhout JA, Josten N, Yamada J, Pan F, Wu S-W, Nguyen PL, Panagiotakos G, Inoue YU, Egusa SF, Volgyi B, et al. 2011. Cadherin-6 mediates axon-target matching in a non-image-forming visual circuit. *Neuron* **71:** 632–639. doi:10.1016/j.neuron.2011.07.006

Osterhout JA, El-Danaf RN, Nguyen PL, Huberman AD. 2014. Birthdate and outgrowth timing predict cellular mechanisms of axon target matching in the developing visual pathway. *Cell Rep* **8:** 1006–1017. doi:10.1016/j.celrep.2014.06.063

Osterhout JA, Stafford BK, Nguyen PL, Yoshihara Y, Huberman AD. 2015. Contactin-4 mediates axon-target specificity and functional development of the accessory optic system. *Neuron* **86:** 985–999. doi:10.1016/j.neuron.2015.04.005

Peng J, Fabre PJ, Dolique T, Swikert SM, Kermasson L, Shimogori T, Charron F. 2018. Sonic Hedgehog is a remotely produced cue that controls axon guidance trans-axonally at a midline choice point. *Neuron* **97:** 326–340.e4. doi:10.1016/j.neuron.2017.12.028

Peng YR, Shekhar K, Yan W, Herrmann D, Sappington A, Bryman GS, van Zyl T, Do MTH, Regev A, Sanes JR. 2019. Molecular classification and comparative taxonomics of foveal and peripheral cells in primate retina. *Cell* **176:** 1222–1237.e22. doi:10.1016/j.cell.2019.01.004

Penn AA, Riquelme PA, Feller MB, Shatz CJ. 1998. Competition in retinogeniculate patterning driven by spontaneous activity. *Science* **279:** 2108–2112. doi:10.1126/science.279.5359.2108

Petros TJ, Bryson JB, Mason C. 2010. Ephrin-B2 elicits differential growth cone collapse and axon retraction in retinal ganglion cells from distinct retinal regions. *Dev Neurobiol* **70:** 781–794. doi:10.1002/dneu.20821

Cold Spring Harbor Perspectives in Biology
www.cshperspectives.org

Pfeiffenberger C, Cutforth T, Woods G, Yamada J, Rentería RC, Copenhagen DR, Flanagan JG, Feldheim DA. 2005. Ephrin-As and neural activity are required for eye-specific patterning during retinogeniculate mapping. *Nat Neurosci* **8:** 1022–1027. doi:10.1038/nn1508

Pfeiffenberger C, Yamada J, Feldheim DA. 2006. Ephrin-As and patterned retinal activity act together in the development of topographic maps in the primary visual system. *J Neurosci* **26:** 12873–12884. doi:10.1523/JNEUROSCI.3595-06.2006

Piscopo DM, El-Danaf RN, Huberman AD, Niell CM. 2013. Diverse visual features encoded in mouse lateral geniculate nucleus. *J Neurosci* **33:** 4642–4656. doi:10.1523/JNEUROSCI.5187-12.2013

Plas DT, Lopez JE, Crair MC. 2005. Pretarget sorting of retinocollicular axons in the mouse. *J Comp Neurol* **491:** 305–319. doi:10.1002/cne.20694

Prieur DS, Rebsam A. 2017. Retinal axon guidance at the midline: chiasmatic misrouting and consequences. *Dev Neurobiol* **77:** 844–860. doi:10.1002/dneu.22473

Quattrochi LE, Stabio ME, Kim I, Ilardi MC, Fogerson PM, Leyrer ML, Berson DM. 2019. The M6 cell: A small-field bistratified photosensitive retinal ganglion cell. *J Comp Neurol* **527:** 297–311. doi:10.1002/cne.24556

Rafols JA, Valverde F. 1973. The structure of the dorsal lateral geniculate nucleus in the mouse. A golgi and electron microscopic study. *J Comp Neurol* **150:** 303–332. doi:10.1002/cne.901500305

Read JCA. 2021. Binocular vision and stereopsis across the animal kingdom. *Annu Rev Vis Sci* **7:** 389–415. doi:10.1146/annurev-vision-093019-113212

Reese BE. 1988. "Hidden lamination" in the dorsal lateral geniculate nucleus: the functional organization of this thalamic region in the rat. *Brain Res* **472:** 119–137. doi:10.1016/0165-0173(88)90017-3

Reinhard K, Li C, Do Q, Burke EG, Heynderickx S, Farrow K. 2019. A projection specific logic to sampling visual inputs in mouse superior colliculus. *eLife* **8:** e50697. doi:10.7554/eLife.50697

Rheaume BA, Jereen A, Bolisetty M, Sajid MS, Yang Y, Renna K, Sun L, Robson P, Trakhtenberg EF. 2018. Single cell transcriptome profiling of retinal ganglion cells identifies cellular subtypes. *Nat Commun* **9:** 2759. doi:10.1038/s41467-018-05134-3

Rhoades RW, Chalupa LM. 1978. Functional properties of the corticotectal projection in the golden hamster. *J Comp Neurol* **180:** 617–634. doi:10.1002/cne.901800312

Rivlin-Etzion M, Zhou K, Wei W, Elstrott J, Nguyen PL, Barres BA, Huberman AD, Feller MB. 2011. Transgenic mice reveal unexpected diversity of on-off direction-selective retinal ganglion cell subtypes and brain structures involved in motion processing. *J Neurosci* **31:** 8760–8769. doi:10.1523/JNEUROSCI.0564-11.2011

Rivlin-Etzion M, Grimes WN, Rieke F. 2018. Flexible neural hardware supports dynamic computations in retina. *Trends Neurosci* **41:** 224–237. doi:10.1016/j.tins.2018.01.009

Rodger J, Dunlop SA, Beazley LD. 1998. The ipsilateral retinal projection in the fat-tailed dunnart, *Sminthopsis crassicaudata*. *Vis Neurosci* **15:** 677–684. doi:10.1017/S095252389815407X

Román Rosón M, Bauer Y, Kotkat AH, Berens P, Euler T, Busse L. 2019. Mouse dLGN receives functional input from a diverse population of retinal ganglion cells with limited convergence. *Neuron* **102:** 462–476.e8. doi:10.1016/j.neuron.2019.01.040

Rompani SB, Müllner FE, Wanner A, Zhang C, Roth CN, Yonehara K, Roska B. 2017. Different modes of visual integration in the lateral geniculate nucleus revealed by single-cell-initiated transsynaptic tracing. *Neuron* **93:** 767–776.e6. doi:10.1016/j.neuron.2017.01.028

Rossi FM, Pizzorusso T, Porciatti V, Marubio LM, Maffei L, Changeux JP. 2001. Requirement of the nicotinic acetylcholine receptor β2 subunit for the anatomical and functional development of the visual system. *Proc Natl Acad Sci* **98:** 6453–6458. doi:10.1073/pnas.101120998

Rousso DL, Qiao M, Kagan RD, Yamagata M, Palmiter RD, Sanes JR. 2016. Two pairs of ON and OFF retinal ganglion cells are defined by intersectional patterns of transcription factor expression. *Cell Rep* **15:** 1930–1944. doi:10.1016/j.celrep.2016.04.069

Russell AL, Dixon KG, Triplett JW. 2022. Diverse modes of binocular interactions in the mouse superior colliculus. *J Neurophysiol* **127:** 913–927. doi:10.1152/jn.00526.2021

Sabbah S, Gemmer JA, Bhatia-Lin A, Manoff G, Castro G, Siegel JK, Jeffery N, Berson DM. 2017. A retinal code for motion along the gravitational and body axes. *Nature* **14:** 5267.

Salay LD, Huberman AD. 2021. Divergent outputs of the ventral lateral geniculate nucleus mediate visually evoked defensive behaviors. *Cell Rep* **37:** 109792. doi:10.1016/j.celrep.2021.109792

Sánchez-Arrones L, Nieto-Lopez F, Sánchez-Camacho C, Carreres MI, Herrera E, Okada A, Bovolenta P. 2013. Shh/Boc signaling is required for sustained generation of ipsilateral projecting ganglion cells in the mouse retina. *J Neurosci* **33:** 8596–8607. doi:10.1523/JNEUROSCI.2083-12.2013

Savier E, Eglen SJ, Bathélémy A, Perraut M, Pfrieger FW, Lemke G, Reber M. 2017. A molecular mechanism for the topographic alignment of convergent neural maps. *eLife* **6:** e20470. doi:10.7554/eLife.20470

Schiller PH, Stryker M. 1972. Single-unit recording and stimulation in superior colliculus of the alert rhesus monkey. *J Neurophysiol* **35:** 915–924. doi:10.1152/jn.1972.35.6.915

Schmitt AM, Shi J, Wolf AM, Lu CC, King LA, Zou Y. 2006. Wnt–Ryk signalling mediates medial–lateral retinotectal topographic mapping. *Nature* **439:** 31–37. doi:10.1038/nature04334

Seabrook TA, El-Danaf RN, Krahe TE, Fox MA, Guido W. 2013. Retinal input regulates the timing of corticogeniculate innervation. *J Neurosci* **33:** 10085–10097. doi:10.1523/JNEUROSCI.5271-12.2013

Seabrook TA, Burbridge TJ, Crair MC, Huberman AD. 2017. Architecture, function, and assembly of the mouse visual system. *Annu Rev Neurosci* **40:** 499–538. doi:10.1146/annurev-neuro-071714-033842

Siegert S, Scherf BG, Del Punta K, Didkovsky N, Heintz N, Roska B. 2009. Genetic address book for retinal cell types. *Nat Neurosci* **12:** 1197–1204. doi:10.1038/nn.2370

Simon DK, O'Leary DD. 1992. Development of topographic order in the mammalian retinocollicular projection. *J*

*Neurosci* **12:** 1212–1232. doi:10.1523/JNEUROSCI.12-04-01212.1992

Simpson JI. 1984. The accessory optic system. *Annu Rev Neurosci* **7:** 13–41. doi:10.1146/annurev.ne.07.030184.000305

Slavi N, Balasubramanian R, Lee MA, Liapin M, Oaks-Leaf R, Peregrin J, Potenski A, Troy CM, Ross ME, Herrera E, et al. 2023. CyclinD2-mediated regulation of neurogenic output from the retinal ciliary margin is perturbed in albinism. *Neuron* **111:** 49–64.e5. doi:10.1016/j.neuron.2022.10.025

Sparks DL, Lee C, Rohrer WH. 1990. Population coding of the direction, amplitude, and velocity of saccadic eye movements by neurons in the superior colliculus. *Cold Spring Harb Symp Quant Biol* **55:** 805–811. doi:10.1101/SQB.1990.055.01.075

Stafford BK, Sher A, Litke AM, Feldheim DA. 2009. Spatial-temporal patterns of retinal waves underlying activity-dependent refinement of retinofugal projections. *Neuron* **64:** 200–212. doi:10.1016/j.neuron.2009.09.021

Su J, Haner CV, Imbery TE, Brooks JM, Morhardt DR, Gorse K, Guido W, Fox MA. 2011. Reelin is required for class-specific retinogeniculate targeting. *J Neurosci* **31:** 575–586. doi:10.1523/JNEUROSCI.4227-10.2011

Su J, Sabbagh U, Liang Y, Olejníková L, Dixon KG, Russell AL, Chen J, Pan YA, Triplett JW, Fox MA. 2021. A cell-ECM mechanism for connecting the ipsilateral eye to the brain. *Proc Natl Acad Sci* **118:** e2104343118. doi:10.1073/pnas.2104343118

Suetterlin P, Drescher U. 2014. Target-independent ephrina/EphA-mediated axon-axon repulsion as a novel element in retinocollicular mapping. *Neuron* **84:** 740–752. doi:10.1016/j.neuron.2014.09.023

Sun LO, Brady CM, Cahill H, Al-Khindi T, Sakuta H, Dhande OS, Noda M, Huberman AD, Nathans J, Kolodkin AL. 2015. Functional assembly of accessory optic system circuitry critical for compensatory eye movements. *Neuron* **86:** 971–984. doi:10.1016/j.neuron.2015.03.064

Thompson AD, Picard N, Min L, Fagiolini M, Chen C. 2016. Cortical feedback regulates feedforward retinogeniculate refinement. *Neuron* **91:** 1021–1033. doi:10.1016/j.neuron.2016.07.040

Tien NW, Vitale C, Badea TC, Kerschensteiner D. 2022. Layer-specific developmentally precise axon targeting of transient suppressed-by-contrast retinal ganglion cells (tSbC RGCs). *J Neurosci* **42:** 7213–7221. doi:10.1523/JNEUROSCI.2332-21.2022

Tiriac A, Feller MB. 2022. Roles of visually evoked and spontaneous activity in the development of retinal direction selectivity maps. *Trends Neurosci* **45:** 529–538. doi:10.1016/j.tins.2022.04.002

Tiriac A, Smith BE, Feller MB. 2018. Light prior to eye opening promotes retinal waves and eye-specific segregation. *Neuron* **100:** 1059–1065.e4. doi:10.1016/j.neuron.2018.10.011

Tiriac A, Bistrong K, Pitcher MN, Tworig JM, Feller MB. 2022. The influence of spontaneous and visual activity on the development of direction selectivity maps in mouse retina. *Cell Rep* **38:** 110225. doi:10.1016/j.celrep.2021.110225

Tomar M, Beros J, Meloni B, Rodger J. 2023. Interactions between guidance cues and neuronal activity: therapeutic insights from mouse models. *Int J Mol Sci* **24:** 6966. doi:10.3390/ijms24086966

Tran NM, Shekhar K, Whitney IE, Jacobi A, Benhar I, Hong G, Yan W, Adiconis X, Arnold ME, Lee JM, et al. 2019. Single-cell profiles of retinal ganglion cells differing in resilience to injury reveal neuroprotective genes. *Neuron* **104:** 1039–1055.e12. doi:10.1016/j.neuron.2019.11.006

Triplett JW, Feldheim DA. 2012. Eph and ephrin signaling in the formation of topographic maps. *Semin Cell Dev Biol* **23:** 7–15. doi:10.1016/j.semcdb.2011.10.026

Triplett JW, Owens MT, Yamada J, Lemke G, Cang J, Stryker MP, Feldheim DA. 2009. Retinal input instructs alignment of visual topographic maps. *Cell* **139:** 175–185. doi:10.1016/j.cell.2009.08.028

Triplett JW, Phan A, Yamada J, Feldheim DA. 2012. Alignment of multimodal sensory input in the superior colliculus through a gradient-matching mechanism. *J Neurosci* **32:** 5264–5271. doi:10.1523/JNEUROSCI.0240-12.2012

Tsai NY, Wang F, Toma K, Yin C, Takatoh J, Pai EL, Wu K, Matcham AC, Yin L, Dang EJ, et al. 2022. Trans-Seq maps a selective mammalian retinotectal synapse instructed by nephronectin. *Nat Neurosci* **25:** 659–674. doi:10.1038/s41593-022-01068-8

Usrey WM, Alitto HJ. 2015. Visual functions of the thalamus. *Annu Rev Vis Sci* **1:** 351–371. doi:10.1146/annurev-vision-082114-035920

Voufo C, Chen AQ, Smith BE, Yan R, Feller MB, Tiriac A. 2023. Circuit mechanisms underlying embryonic retinal waves. *eLife* **12:** e81983. doi:10.7554/eLife.81983

Walls GL. 1942. *The vertebrate eye and its adaptive radiation*. Cranbrook Institute of Science, Bloomfield Hills, MI.

Walmsley L, Brown TM. 2015. Eye-specific visual processing in the mouse suprachiasmatic nuclei. *J Physiol* **593:** 1731–1743. doi:10.1113/jphysiol.2014.288225

Wang Q, Burkhalter A. 2013. Stream-related preferences of inputs to the superior colliculus from areas of dorsal and ventral streams of mouse visual cortex. *J Neurosci* **33:** 1696–1705. doi:10.1523/JNEUROSCI.3067-12.2013

Wang F, Li E, De L, Wu Q, Zhang Y. 2021. OFF-transient α RGCs mediate looming triggered innate defensive response. *Curr Biol* **31:** 2263–2273.e3. doi:10.1016/j.cub.2021.03.025

Warland DK, Huberman AD, Chalupa LM. 2006. Dynamics of spontaneous activity in the fetal macaque retina during development of retinogeniculate pathways. *J Neurosci* **26:** 5190–5197. doi:10.1523/JNEUROSCI.0328-06.2006

Warwick RA, Kaushansky N, Sarid N, Golan A, Rivlin-Etzion M. 2018. Inhomogeneous encoding of the visual field in the mouse retina. *Curr Biol* **28:** 655–665.e3. doi:10.1016/j.cub.2018.01.016

Williams SE, Mann F, Erskine L, Sakurai T, Wei S, Rossi DJ, Gale NW, Holt CE, Mason CA, Henkemeyer M. 2003. Ephrin-B2 and EphB1 mediate retinal axon divergence at the optic chiasm. *Neuron* **39:** 919–935. doi:10.1016/j.neuron.2003.08.017

Williams SE, Grumet M, Colman DR, Henkemeyer M, Mason CA, Sakurai T. 2006. A role for Nr-CAM in the patterning of binocular visual pathways. *Neuron* **50:** 535–547. doi:10.1016/j.neuron.2006.03.037

Cold Spring Harbor Perspectives in Biology
www.cshperspectives.org

Wong RO. 1999. Retinal waves and visual system development. *Annu Rev Neurosci* **22:** 29–47. doi:10.1146/annurev.neuro.22.1.29

Wurtz RH, Goldberg ME. 1972. The role of the superior colliculus in visually-evoked eye movements. *Bibl Ophthalmol* **82:** 149–158.

Yates PA, Roskies AL, McLaughlin T, O'Leary DD. 2001. Topographic-specific axon branching controlled by ephrin-As is the critical event in retinotectal map development. *J Neurosci* **21:** 8548–8563. doi:10.1523/JNEUROSCI.21-21-08548.2001

Zeng H, Sanes JR. 2017. Neuronal cell-type classification: challenges, opportunities and the path forward. *Nat Rev Neurosci* **18:** 530–546. doi:10.1038/nrn.2017.85

Zhang J, Ackman JB, Xu HP, Crair MC. 2011. Visual map development depends on the temporal pattern of binocular activity in mice. *Nat Neurosci* **15:** 298–307. doi:10.1038/nn.3007

Zhao X, Liu M, Cang J. 2014. Visual cortex modulates the magnitude but not the selectivity of looming-evoked responses in the superior colliculus of awake mice. *Neuron* **84:** 202–213. doi:10.1016/j.neuron.2014.08.037

Zhao ZD, Chen Z, Xiang X, Hu M, Xie H, Jia X, Cai F, Cui Y, Chen Z, Qian L, et al. 2019. Zona incerta GABAergic neurons integrate prey-related sensory signals and induce an appetitive drive to promote hunting. *Nat Neurosci* **22:** 921–932. doi:10.1038/s41593-019-0404-5

Cold Spring Harbor Perspectives in Biology
www.cshperspectives.org

# Mapping the Retina onto the Brain

Daniel Kerschensteiner and Marla B. Feller

*Cold Spring Harb Perspect Biol* published online December 5, 2023